PACIFIC COLLECTION
RECEIVED 25/01/07

THE UNIVERSITY OF THE SOUTH PACIFIC
LIBRARY

DIGITAL THESES PROJECT

Author Statement of Accessibility- Part 2- Permission for Internet Access

Name of Candidate : JAYSHREE LAL

Degree : MASTER OF SCIENCE

Department/School : The University of the South Pacific

Institution/University : THE UNIVERSITY OF THE SOUTH PACIFIC

Thesis Title : COMPACT ANTENNAS FOR MOBILE COMMUNICATIONS.

Date of completion of requirements for award : ----------

1. I authorise the University to make this thesis available on the Internet for access by USP authorised users. Yes/~~No~~

2. I authorise the University to make this thesis available on the Internet under the International digital theses project Yes/~~No~~

Signed: JG

Date: 18/12/06

Contact Address

Indian College,
Suva.
Ph: 9269891
e-mail : jayshri_lal@yahoo.co.uk

Permanent Address

P.O. Box 7063
Nasiny.
e-mail: jayshri_lal@yahoo.co.uk

COMPACT ANTENNAS FOR MOBILE COMMUNICATIONS

by

Jayshree Lal

Thesis submitted in fulfillment of the requirements for the degree

Master of Science

in the

School of Engineering and Physics
UNIVERSITY OF THE SOUTH PACIFIC

June 2006

DECLARATION OF ORIGINALITY

I, Jayshree Lal, declare that this thesis is my own work, and that to the best of my knowledge is original, except as acknowledged in the text. This thesis has not been submitted for the award of any other degree at this or any other institution.

Jayshree Lal

ABSTRACT

Size miniaturization of microstrip patch antennas is one of those antenna research fields, which is becoming essential in many practical applications. The demand for smaller mobile handsets, cordless phones, global position satellites and other next – generation wireless terminals has placed a huge responsibility on the communication engineers to design and develop compact antennas such that the size of the mobile terminals can be reduced as well.

The objective of this thesis is to investigate small patch antennas suitable for mobile communications. There are currently many size reduction techniques available in the open literature. In this research, some of those techniques were explored to determine the best ways of reducing the antenna real estate. Consequently, a compact Y-shaped stacked antenna was designed. This antenna is easy to manufacture and could be used in mobile terminals. Using the techniques explored in the open literature, another compact printed antenna was then designed. It is F-shaped and has a foam material sandwiched between the ground plane and the radiator plane to improve its bandwidth performance. This antenna could be used for PCS applications. An interleaved F-shaped and cross-shaped stacked antenna was then designed using the technique of shorting pins and slots. This compact design could find applications in systems such as DCS 1800 (1805 MHz-1880 MHz), Digital European Cordless Telephone (1880 MHz-1990 MHz), Personal Handy Phone System (1895 MHz-1918 MHz) and PCS systems. The fourth compact stacked antenna configuration was designed using the common size reduction techniques such as slots and shorting pins. The antenna uses a square shaped print for the top layer

and has a cross-shaped bottom layer. The top radiator uses semi circular grooves to maximize current path such that miniaturization is achieved. Finally, we have used the patch configuration from the first two antennas to design a final Y-shaped and interleaved F-shaped stacked antenna. The antenna has a simple configuration due to the position of the shorting pins and the probe pin.

Chapter 4 of this dissertation deals with the simulation results of the antennas designed above. The impedance bandwidth of each antenna is determined and the percentage size reduction is calculated compared to a conventional microstrip patch antenna (reference antenna). The radiation patterns of these antennas are also studied. The Y-shaped stacked antenna has a bandwidth of 10.2 %. The antenna real estate decreased by a factor of 3 compared to the conventional patch antenna. A simulated bandwidth of (VSWR >2) 7 % was achieved for the interleaved F-shaped antenna. The antenna is 65 % smaller than the reference antenna. To validate the designs using the *IE3D simulator* software, the interleaved F-shaped antenna was fabricated and tested. The return loss bandwidths of the simulated and measured results (VSWR >3) are in good agreement with each other in the L band of the frequency spectrum. However, degradation below the –5 dB return loss results can be attributed to fabrication tolerances when manufacturing the antenna. An impedance bandwidth of 10.5 % was achieved for the stacked interleaved F-shaped and cross- shaped antenna. This is a relatively high bandwidth. The antenna real estate decreased by 65 %. The fourth design has a bandwidth of 8.4 % and is again 65 % smaller than the reference antenna. In the case of the last design, a 63% patch size reduction from the conventional probe fed rectangular patch antenna has been observed whilst the simulated antenna bandwidth is 8.15 %.

ACKNOWLEDGMENTS

I would like to express my gratitude to all those who have helped me in every possible way to successfully complete this thesis. Firstly I would like to thank the School of Engineering & Physics, the University of the South Pacific, for accepting me in its Graduate Assistant scheme. It is because of this scheme that I have been able to undertake a Master of Science Degree.

I am deeply indebted to my supervisor, Dr Hing Kiu Kan, from the School of Engineering & Physics. His constant help, suggestions, ideas and encouragement have helped me throughout this research work. Without his supervision I would not have been able to complete this thesis the way I have. He has also helped me on how to write research papers and it is with his help that I was able to publish my research work in *Microwave and Optical Technology Letters* and the *2005 APMC Conference Proceedings*.

A kind acknowledgement goes to Dr. Rowe from Royal Melbourne Institute of Technology for testing my research design and sending over the results. It is through his kind help that my design was tested using the proper facilities.

I am also grateful to my parents and family in Lautoka, my in-laws and my God who have blessed me throughout this work. Finally, I would like to give my special thanks to my husband, Vinesh, whose constant support, love and patience has enabled me to complete this thesis. I would like to take this opportunity to tell him how much his love and support has helped me to go through all the difficult times during this research work.

PUBLICATIONS

- Lal, J., and Kan, H. K., "Cross-shaped shorted patch antenna", *2005 Proc. Asia Pacific Microwave Conference*, Suzhou, China, Vol 3, pp. 1 – 4, December 2005.
- Lal, J., Kan, H. K., Rowe, W. S. T., "F-shaped shorted patch antenna with dual – frequency characteristics", accepted to *Microwave & Optical Technology Letters*, April.
- Lal, J., Kan, H. K., Rowe, W. S. T., and Chung, K. L., "F-shaped shorted patch antenna with dual-frequency characteristics", submitted to *IEEE TENCON* 2006, Hong Kong, May 2006

LIST OF FIGURES

TABLE OF CONTENTS

CHAPTER 1: INTRODUCTION

1.1 Background

An ever-increasing growth of wireless communications has stimulated extensive research in the field of antennas. One major area of wireless communications where there is a rapid growth is the mobile communications. The use of mobile phones is on a rise because it has made communication much easier. Mobile communication antennas should be cheap, easy to manufacture and should be lightweight and robust. Most importantly they should have a low profile characteristic and be as compact as possible so that it can be aesthetically embedded within the handset. It is because of these reasons that research on mobile communication antennas are increasing. One particular class of antenna that meets such requirement is the microstrip patch antenna. The development of microstrip patch antennas has made serious advancements in the 1970's and is currently probably the most active field in antenna research and development.

Conventional microstrip patch antenna consists of a pair of parallel conducting layers separated by a dielectric medium, referred to as the substrate. The source of radiation is the upper conducting layer known as the patch layer. The lower conducting layer acts as a perfectly reflecting ground plane, bouncing the energy back through the substrate and into the free space [1]. Figure 1.1 shows the general configuration of a conventional rectangular microstrip patch antenna [2]. Microstrip antennas come in a variety of configuration. Rectangular and circular patches are most common, but any shape that possesses a reasonably well-defined resonant mode can be used.

There are many interesting electrical and physical properties of microstrip patch antennas. The concentration of currents in the conducting layers is higher than the total current in all the elements; the height of the antenna (most often the direction of maximum radiation) is electrically small; and microstrip patch antennas are always excited at or near resonance. Electrically most patch antennas have a very broad beam because of its small size [3].

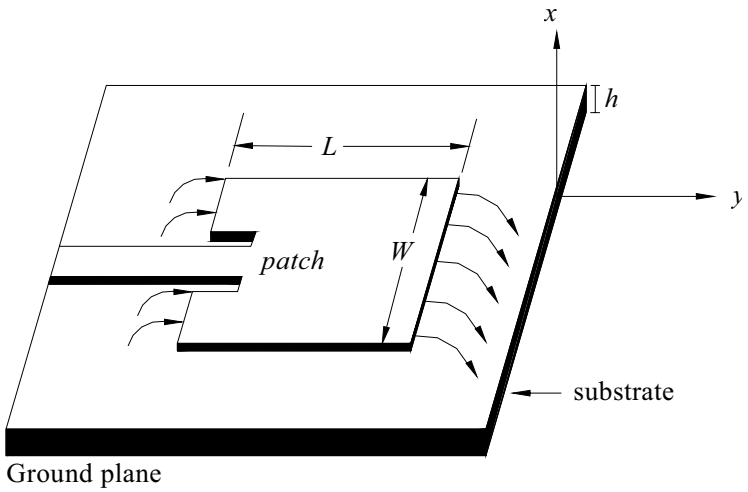

Figure 1.1: Microstrip antenna.

There are many ways to feed the microstrip patch antenna. The most popular methods to feed or transmit electromagnetic energy to a microstrip antenna are: aperture coupling, proximity coupling, microstrip line and coaxial probe [2]. Figure 1.2 shows the different feeding techniques available for microstrip patch antennas. The aperture coupling method as shown in Figure 1.2 (a) consists of two substrates separated by a ground plane. The energy is coupled from a microstrip feed line, through a slot on the ground plane separating the two substrates, to the patch. The amount of coupling is determined by the shape, size and location of the aperture. The microstrip line is etched

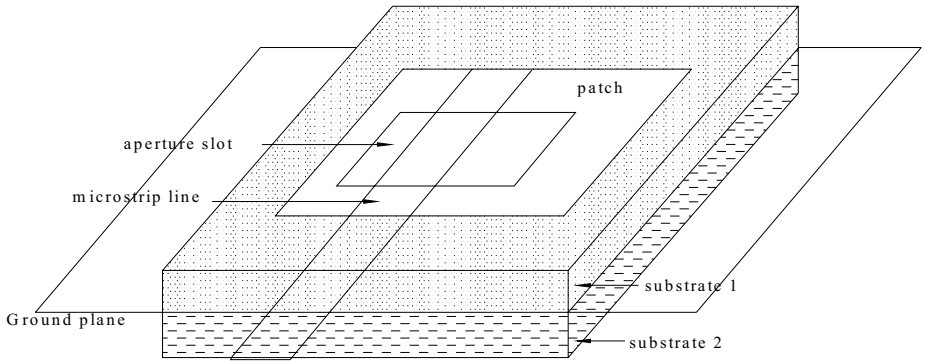

Figure 1.2 (a): Aperture feeding method

on the bottom side of the lower substrate. A high dielectric substrate material is commonly used for the bottom layer and a thick, low dielectric constant substrate for the top layer to optimize the radiation patterns. The substrate electrical parameters, feed line width, slot size and position of the slot can be used to optimize the design. However, this feeding method is the most difficult to fabricate since parameters such as aperture size, width and length of the microstrip feed line, size of the ground plane and thickness of the dielectric substrate material has to be determined correctly for the antenna to operate at the desired frequency.

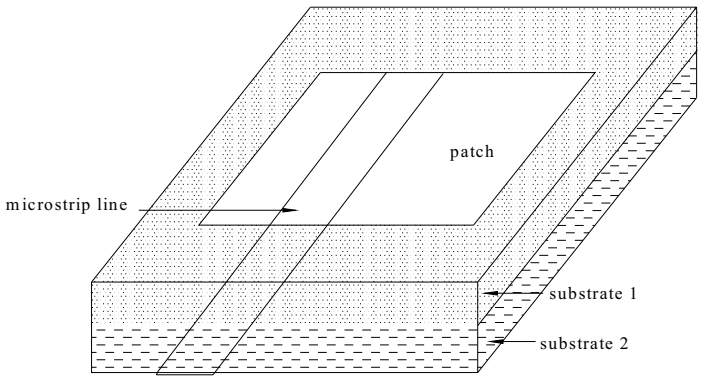

Figure 1.2(b): Proximity feeding method

The proximity coupling method is shown in Figure 1.2 (b). As it can be seen from the figure proximity coupling method utilizes two dielectric substrates such that the feed line is located between the two substrates with the radiating patch on top of the upper substrate. This type of feeding technique is also called the electromagnetic coupling scheme because it includes a dielectric substrate for the microstrip feed and another suspended dielectric layer for the active patch. Matching can be achieved by controlling the length of the feed line and the linear dimensions of the patch. The increased overall thickness of the antenna can also enable an increase in the overall bandwidth of the antenna. This type of feeding method is difficult to fabricate because of the two dielectric layers, which needs careful alignment. The thickness of the antenna also increases the overall size of the antenna.

The two easiest feeding methods are the microstrip feed line and the probe feeding technique, which are shown in Figure 1.2 (c) and Figure 1.2 (d), respectively. In the case of the microstrip feed line, a conducting strip is etched on the same substrate as the main antenna element. The strip is connected directly to the patch edge and is much smaller in width compared to the patch. This is an easy feeding technique but has several disadvantages such as undesired cross polarization and the introduction of surface waves when thicker dielectric substrate are used leading to increased overall antenna size. With respect to the coaxial probe feeding method, the inner conductor of the coax is connected to the radiator whilst the outer conductor is connected to the ground plane. The probe feed has a number of desirable characteristics that makes it very suitable for applications in the wireless communications field. Since the probe is directly connected to the patch, the antenna structure is quite robust. This method is also less prone to alignment errors

and less spurious radiation from the feed network since it is separated from the patch. The point of excitation is also adjustable for impedance matching. Therefore inorder to reduce the complexity and size of the antennas, the antenna designs involved in this research will be utilizing the coaxial feeding technique.

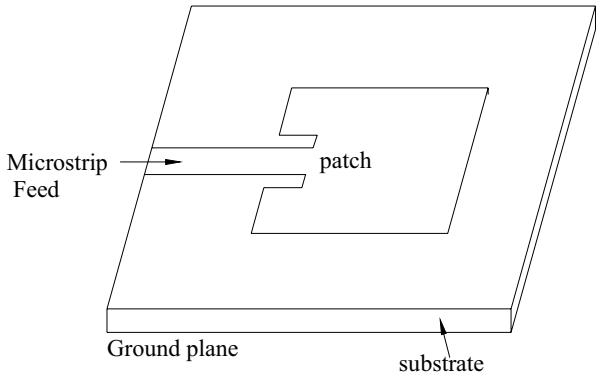

Figure 1.2(c): Microstrip line feeding method

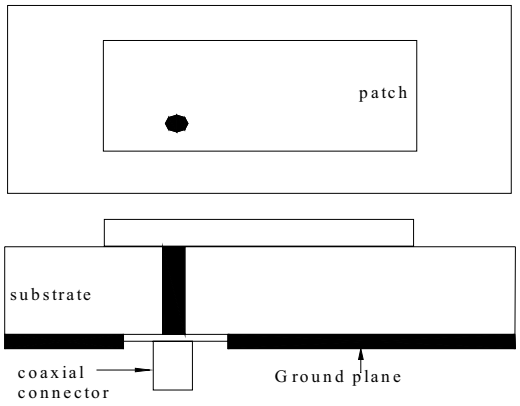

Figure 1.2(d): Coaxial probe feeding method

After careful selection of the feed type and a reasonably shaped patch, a microstrip patch antenna can be used for various wireless applications. The antenna should be further reduced in size so that it can be aesthetically embedded with portable wireless device. Microstrip antennas in its conventional form are too large for practical wireless applications. Therefore, communications engineers are constantly working on new designs such that aesthetically pleasing antennas are brought into the market. The aim of this thesis is therefore to review the size reduction methods available in the open literature with respect to reducing the size of microstrip patch antennas. The second aim of this thesis is to analyze the size reduction techniques reviewed above to determine which size reduction method gives the most and least percentage reduction and bandwidth. The third aim is to develop new compact probe-fed microstrip patch antenna with reasonable impedance bandwidth based on the literature study performed, that can fulfill the requirements of modern day mobile communications. The PCS communication system, for example, requires a bandwidth of several percentages around the resonant frequency. The final aim of this thesis is to fabricate at least one new design and test it using the proper facilities to validate the design of the antenna using the software package. In the next section, the objectives of this study are formulated in more detail.

1.2 Objectives

As mentioned in the previous section, there are four main objectives to this thesis. This includes the study of the size reduction techniques available in the open literature, the analyses of these size reduction techniques using a software package, the design of new compact patch antennas viable for mobile communications and the fabrication and

testing of at least one antenna design. The following bullet point discusses the objectives in detail.

- The first objective of this thesis is to study some common size reduction techniques available in the literature. Modern mobile communication systems currently demand even smaller patch antennas due to the constant decrease in the overall size of the mobile handsets and other portable devices that operate in the L band frequency range. Apart from having an antenna size that is small the communication system usually demands a bandwidth of 5% or more for the antenna to work effectively. Hence a literature survey on some of the available bandwidth enhancement techniques will be conducted. The scope of the literature review mentioned in this bullet point will be limited to rectangular probe fed antennas.

- The second objective is to analyze various methods of reducing the patch antennas by using a software package and to determine the best methods of reducing the dimensions of a patch antenna. From this study, it will then assist in determining which techniques should be utilized in this research work for the design of new patch antennas that can satisfy the space restriction commonly associated with wireless devices.

- The third objective of this thesis is to utilize the size reduction techniques determined from the literature review mentioned above to design new compact patch antennas. Numerous CAD simulations utilizing an electromagnetic

simulator IE3D will be carried out until a satisfactory result, in terms of the return loss and radiation pattern is achieved. The resonant frequencies of these antennas will be designed at L and S band of the frequency spectrum. All the antennas will be coaxially fed with the basic shape of a rectangle.

- The final and the most important objective of this research work will be the fabrication and testing of at least one antenna to validate the design of the antenna using the software package. The measured results will verify the simulated results and enable us to determine whether these antennas can indeed be used for practical wireless portable applications.

1.3 Overview of the Thesis

In this chapter, we have briefly looked at the background of microstrip patch antennas. The advantages of patch antennas were discussed with respect to its application in wireless communications. The different feeding methods that can be used to couple power to the printed antennas are also reviewed in this chapter. Merits and problems of each of the feeding methods have also been discussed. It was concluded that coaxial feeding method was chosen over the other feeding methods due to its many advantages. These advantages include less alignment errors, reduced spurious radiation from the feed network and an adjustable point of excitation for impedance matching. After a careful research on microstrip patch antenna, the objectives of this thesis have been presented. The original contributions of this thesis will also be discussed in this chapter. An overview of the remaining chapters is then discussed.

Chapter 2 presents several analyses on the size reduction methods commonly utilized in the open literature. Several size reduction techniques will be discussed which have already been used to design compact antennas for mobile communications. To improve the understanding of these techniques, several of the most common techniques using *Zeland's IE3D simulation package* [4] are analyzed. After numerous simulations it was concluded that the use of shorting pins and slots are the easiest, simplest and most effective methods of reducing patch antennas, especially in terms of manufacturing cost and fabrication tolerance. It is well known that the reduction in antenna size is achieved at the cost of reduced bandwidth. Therefore, bandwidth enhancement techniques for printed antennas will then be investigated to alleviate the reduction in bandwidth and will be presented in this section.

In Chapter 3, the literature review and analysis performed in the previous chapter is utilized to design five new compact antennas suitable for mobile communications, all of which are operational in the L and S band frequency range. All the designs are a result of numerous simulations using *Zeland's IE3D simulation package*. Firstly a reduced size stacked Y-shaped printed antenna will be presented in section 3.2. The reduction technique and the bandwidth enhancement technique for this antenna will be presented. This will be followed by a brief discussion on its degrees of freedom in designing the antenna. An interleaved F-shaped antenna will be presented in section 3.3. This design utilizes shorting pins and slots to reduce the size of conventional rectangular antennas. Design variables of the new interleaved F-shaped antenna are also presented in this sub-section. A third design is presented in section 3.4. It has an interleaved F-shaped antenna as the top radiator and a cross-shaped print conductor for the bottom layer. The new

antenna configuration and its degrees of freedom will be presented in this section. An antenna with a cross-shaped bottom layer is again presented in section 3.5. The top layer, however, is square shaped. This section will discuss the design and configuration of this new antenna. The simulation results will be presented with respect to the design variables of the antenna to determine its effects on the antenna size and its bandwidth. Lastly, a stacked antenna will be presented in section 3.6. In this section a Y-shaped top layer and an interleaved F-shaped bottom layer is used. This design was inspired from the first two designs discussed above.

Chapter 4 presents simulated results of the antennas designed and discussed in chapter 3. One of the simulated antennas designed will be fabricated and tested experimentally. This will then be compared with the simulation results and discussed. The results will be discussed in terms of its return loss characteristics and radiation patterns.

Chapter 5 summarizes the work presented in this thesis. Suggestions for future work will also be presented.

1.4 Original Contributions

The following bullet points describe the major contributions of this thesis.

- A small Y-shaped patch antenna in a stacked configuration. The top layer of this antenna has a Y-shaped patch. A parasitic ring of thickness 1 mm encloses this Y-shaped patch. The bottom layer of this antenna is also a Y-shaped patch conductor that has the same dimensions as the top conductor. A similar parasitic ring

encloses the bottom Y-shaped patch. The bottom layer is aligned exactly to the top layer. A shorting wall connects these two Y-shaped patch layers. Shorting pins and slots are utilized to reduce the size of the overall antenna. A percentage size reduction of 65% and a 10 dB return loss bandwidth 10.2% has been achieved with this configuration.

- A new interleaved F-shaped antenna. The antenna consists of two patches located on the same plane. A straight F-shaped probe-fed patch and an electromagnetically coupled inverted F-shaped patch are interleaved to give a compact configuration. A parasitic ring encloses this interleaved patch conductor. Shorting pins are utilized in both the F-shaped conductors to achieve miniaturization of the antenna. The ground plane and the radiating plane are separated by *Rohacell* foam of thickness 6 mm. The novel design of an interleaved F-shaped antenna resulted in a paper publication [5]. The percentage size reduction is 65% with an impedance bandwidth of 7%.
- A stacked antenna configuration comprising of an interleaved F-shaped conductor as the top layer and a cross-shaped patch as the bottom layer. The top patch layer has the same patch configuration as discussed above. The inverted F-shaped patch is electromagnetically coupled to the straight F-shaped probe-fed patch. Two shorting pins have been utilized to reduce the antenna dimensions. The cross-shaped bottom layer is surrounded by a parasitic ring of thickness 1 mm. The novel design of a cross-shaped antenna resulted in a conference publication [6]. In using this configuration, a 65% size reduction was again achieved with a bandwidth of 10.5%.

- Another new stacked antenna comprises of a square shaped top layer and a cross-shaped bottom layer. The top patch conductor has a square configuration of length 20 mm. Each perimeter of the square print consists of a semi-circular groove cut. These semi–circular grooves increase the current path of the antenna in order to reduce the antenna dimensions. A parasitic ring similar to the other antenna designs is used to improve the antenna bandwidth. The parasitic ring contains two semi-circular grooves. The bottom patch layer has a cross- shape, as discussed above. A shorting pin is used to further reduce the antenna dimensions. The overall percentage reduction was 8.4% and has an overall bandwidth of 8.4%.
- A compact Y-shaped top layer and interleaved F-shaped bottom layer in a stacked configuration. The top radiator is Y-shaped which is enclosed by a parasitic ring of thickness 1 mm. Two shorting pins penetrate from the top layer to the ground plane resulting in the size reduction of the antenna. The bottom patch conductor has an interleaved F- shaped configuration as discussed previously. The percentage size reduction is 63% with an impedance bandwidth of 8.15%.

CHAPTER 2: SMALL PATCH ANTENNAS

2.1 Introduction

Advances in the field of microstrip antennas have led communication engineers to design smaller antennas. The trend is to decrease the weight of the antenna and simultaneously comply with the space restrictions associated with the portable devices. It is because of this trend that compact antenna designs are needed in the communications market. Section 2.2 presents some common literature available for reducing the size of patch antennas. Section 2.3 presents analyses of the size reduction techniques. Through this analysis the percentage reduction in the overall size of the patch antenna is determined. It is found that a decrease in the antenna real estate usually decreases its overall bandwidth and gain. Section 2.4 discusses some common bandwidth enhancement techniques available in the literature for practical applications. Section 2.5 concludes this chapter.

2.2 Overview of the Size Reduction Techniques

There is a great amount of information in the open literature for reducing the size of microstrip patch antennas [7, 8, 9, 10]. In this section, the most common methods of size reduction techniques will be discussed. The entire spectrum of approaches is beyond the scope of this thesis. Some common methods include the use of shorting pins, slots, high dielectric constant substrate materials, chip resistor loading, slow wave structure, and the use of a meandered ground plane.

2.2.1 **Shorting Pin**

Shorting the microstrip patch antenna is one of the most common ways to reduce the antenna size [11]. Figure 2.1 shows a typical patch antenna loaded with one shorting pin. This phenomenon can be explained using electric field components between the patch and the ground plane [12]. The electric field is approximately a cosinusoidal function. It has a maximum value at the edges of the patch, goes to zero at the center and returns to the maximum value again at the other edge of the patch. A short circuit can be placed without affecting its basic operation since the electric field is zero at the middle plan. It is this short circuit that reduces the microstrip patch antenna to half its original length. The electric field components can still be undisturbed if instead of a short circuit, shorting pins are used between the patch and the ground plane. An antenna size reduction of about 89 % has been reported using shorting pins to reduce the antenna real estate [1].

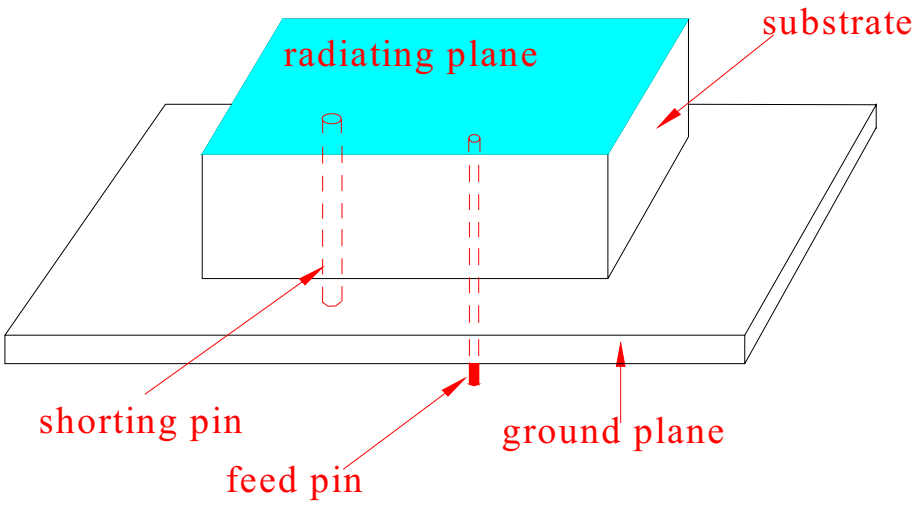

Figure 2.1: Typical shorted patch antenna

There are four degrees of freedom associated with respect to the input impedance variation when a probe fed patch antenna is shorted: radius of the patch, position of the

shorting post relative to the patch edge, the position of the probe feed with respect to the shorting post and the radii of both the feedpin and the shorting pin. Hence the resonant frequency can be controlled using these parameters. One common drawback of using the shorting pin method is that the antenna bandwidth decreases as the size of the antenna reduces. The cross polarization radiation is increased due to the shorting pin loading. The antenna gain is also expected to decrease. In addition, the reduction in the patch size is limited by the distance between the null voltage point in the patch and the patch edge [7].

2.2.2 **Slot**

Embedding slots in the radiating patch can also obtain compact operation of microstrip patch antennas. These embedded slots cause the meandering of the surface current [13]. This action leads to a greatly lengthened current path for a fixed patch linear dimension. Consequently, the antenna fundamental frequency is lowered and thus a large antenna size reduction at a fixed operating frequency can be obtained. Two new design parameters are introduced to tune the antenna impedance and the resonance frequency – the length and width of the slot [14]. Similar behavior results when the radiating patch is meandered [15]. This can be achieved by inserting narrow slits at the patch's non-radiating edges. The meandered patch again lengthens the electrical path such that the fundamental resonant frequency lowers. The antenna dimensions have to be reduced for operation at the desired frequency. Some typical slotted patches are shown in Figure 2.2 [7].

Common disadvantages of using slots to reduce antenna size include an increase in the cross polarization levels [16]. With an increase in the cross polarization levels, a decrease in the gain of the printed antenna is observed, albeit marginally. Additionally,

the slot length is constrained by the initial size of the antenna. The input return loss and port isolation may also degrade. The slotted patch antennas must be carefully designed, taking into consideration the above-mentioned disadvantages.

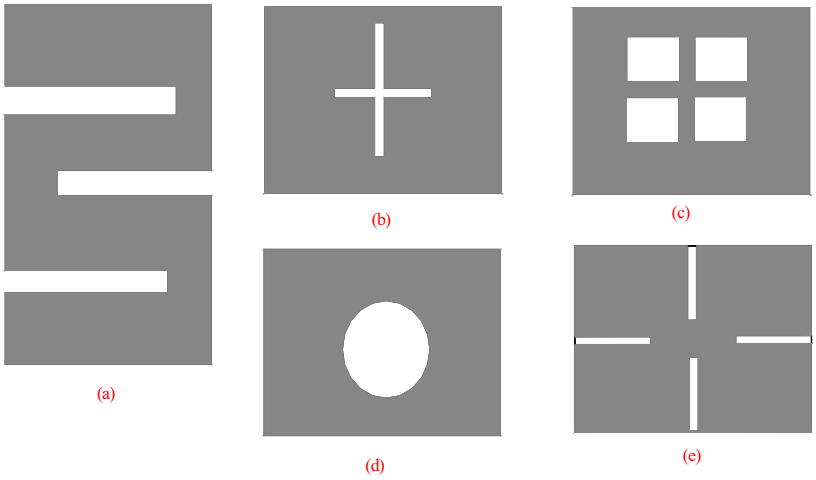

Figure 2.2: Some slotted patches suitable for the design of compact microstrip antennas

2.2.3 **High dielectric substrate material**

The resonant frequency of thin microstrip antenna is given by

$$f = \frac{c}{2L\sqrt{\varepsilon_r}} \qquad (2.1)$$

where c is the speed of light, L is the patch length and ε_r is the dielectric constant of the substrate material. From equation 2.1 it can be seen that the resonant frequency and the dielectric constant of the substrate material are inversely proportional. When the dielectric constant increases, the resonant frequency decreases. A smaller physical antenna length at a fixed frequency can thus result [7]. With the use of higher dielectric constant materials, a greater reduction in the antenna dimensions can be achieved. However, increasing the dielectric constant of the substrate material has some drawbacks

that limit the use of this method. More energy delivered to the antenna is trapped in substrates of high dielectric constant, i.e. surface waves and leaky waves. The efficiency reduces due to these losses in substrate and causes pattern/ polarization degradation. It produces dips near to the maximum and significant sidelobes and cause unwanted coupling [17]. One common solution to overcome this problem is to use the concept of photonic band gap (PBG) structure [18]. Figure 2.3 shows a simple PBG antenna configuration. In this structure the patch antenna is surrounded with a square lattice of small metal pads with grounding vias. With this action substantial surface waves are suppressed. The PBG antenna improves antenna gain, reduces mutual coupling and increases frequency bandwidth as well.

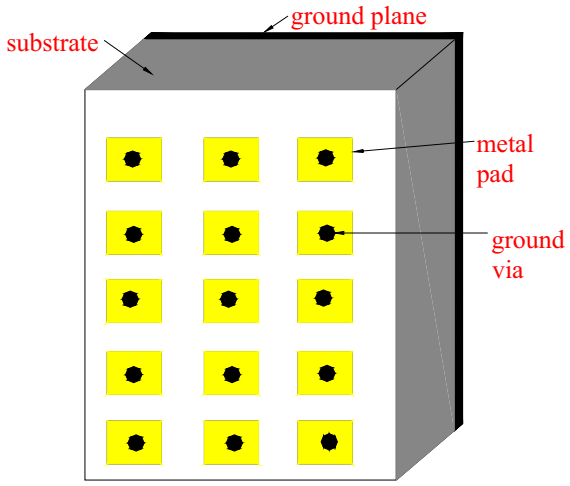

Figure 2.3: A typical PBG antenna configuration

2.2.4 **Chip resistor loading**

A microstrip patch antenna loaded with a chip resistor offers a wider impedance bandwidth compared to the bandwidth achieved with most size reduction methods, such as shorting pins, slots and high dielectric constant material [19]. The reduction obtained with this method is usually much more than what can be obtained with most of the size

reduction techniques. The E-plane radiation pattern is slightly asymmetric due to the excited high current density around the load in the patch antenna.

However, there are some disadvantages associated with the chip resistor loading technique [20]. Firstly, low ohmic resistor values should be used since higher values will increase the ohmic losses. Cross polarization levels increases and the gain decreases mainly due to the ohmic loss of the resistor and the reduced antenna size. In addition, the input impedance is very sensitive to the distance between the loading resistor and the probe feed.

2.2.5 **Slow wave structure**

To implement a slow wave structure (SWS), periodic patterns of slots are cut in the ground plane of a microstrip line [21]. These cuts are small compared to the wavelength and increase the capacitance and inductance. These loadings create a surge in the standing wave of the current. This surge is related to the size reduction of the patch antenna. For example, if the current distribution along the radiating structure can be made to vary from its minimum to its peak value across a lumped element, the microstrip patch antenna can become a quarter wavelength antenna, and hence miniaturization can be achieved [22]. The characteristic impedance is not affected. In [23] the SWS were applied to both the patch and the ground plane. An overall patch size reduction of 50 % was achieved. The antenna configuration used in [23] is shown in Figure 2.4.

The SWS is easy to implement because it does not require any via holes and it is insensitive to alignment errors. Most importantly, as opposed to other size reduction techniques, the bandwidth of the antenna increases. However, like any other size reduction techniques the SWS structure also has disadvantages associated with it. The

back radiation increases from the capacitive gaps in the SWS, hence increasing the losses. The higher bandwidth and size reduction is a compromise with a lower antenna gain.

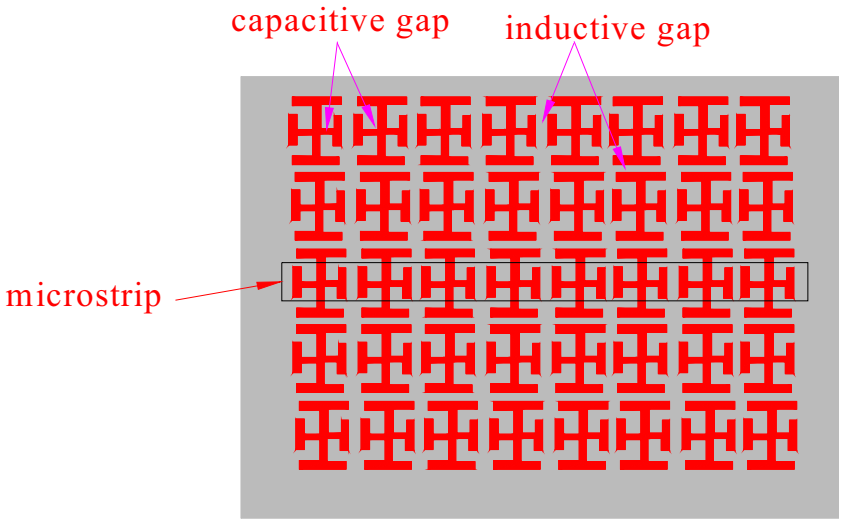

Figure 2.4: SWS implementation

2.2.6 **Reduced ground plane**

Traditional size reduction techniques have only focused on reducing the size of the radiating patch. With the introduction of new design methods, size reduction is also achieved by reducing the size of the supporting ground plane [24]. Ground plane reduction is becoming important given the space restrictions of portable devices.

Reducing the size of the ground plane has two major disadvantages. Firstly, back radiation due to diffraction increases. Diffraction occurs due to the edges of the finite ground plane size and contributes to surface waves, space waves and leaky waves that are not desirable. This effect can be harmful to the user since more radiation will be towards the head. Secondly, the impedance of the antenna changes that affects the matching. Gain of the antenna also decreases with a decrease in the ground plane size.

In [24], one solution to this problem is explored. Cylindrical rings around the patch and the perimeter of the ground are introduced. With this addition, the back radiations are reduced and the gain of the antenna is increased by 5 dB. With this method, an 87 % reduction in the area of the ground plane was obtained.

Similar effects are observed when the ground plane of the microstrip patch antenna is meandered. The gain and impedance bandwidth of the antenna increases. In [7] a size reduction of 56 % is achieved when slots are embedded on the ground plane. The embedded slots, however, introduce backward radiation. The antenna with the meandered ground plane in [7] is shown in Figure 2.5.

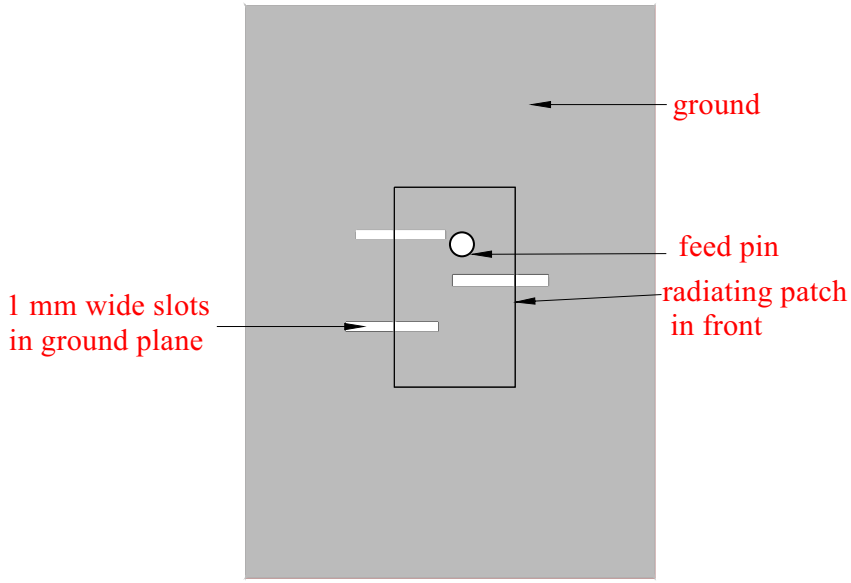

Figure 2.5: Patch antenna with a meandered ground plane (top view)

2.3 Analyses of the Size Reduction Techniques

The analyses of the size reduction techniques have been carried out to determine the percentage of antenna reduction achievable. *Zeland's IE3D EM* simulator has been utilized for this purpose. *IE3D* is full-wave, method-of-moments based electromagnetic

simulator solving the current distribution on 3D and multilayer structures of general shapes. It is an efficient tool for antenna designers.

Note that the reduced ground plane does not have much effect on the antenna impedance bandwidth. More complicated designs, such as placing cylindrical rings around the patch and the perimeter of the ground [24], needs to be incorporated with the reduced plane to counter affect the increase in backward radiation. It was because of this reason that this size reduction technique was not analyzed any further. The above designs can be categorized in three sections, namely, (a) patch meandering (slits, slots), (b)shorting pins (shorting pins, chip resistor loading) and (c) material (high dielectric constant material and slow wave structure). The analyses performed using *Zeland's IE3D* simulator was divided into the three groups mentioned above. The probe feed technique is used to feed the antennas, as explained in section 1.1. *Rogers* 3210 (ε_r = 10.2) is used for the high dielectric substrate material. For all other simulation purposes, *Rogers TMM 4* (ε_r = 4.5) is used. The value of the chip resistor is 2 Ω. The radius of the shorting pin is 2mm and that of the probe pin is 0.486 mm.

The three shapes used to determine percentage reduction, for simulation purposes, were rectangle, triangle and circle. The percentage size reduction and bandwidth was calculated with respect to a reference antenna operating in the L- band spectrum. A reference antenna is one in which no reduction method has been applied to. The dimensions of the reference antennas were as follows: rectangle - 74mm (*Length*) x 32 mm (*Width*), triangle – 98 mm (*Length*) x 86 mm (*height*) and circle – 36 mm (*radius)*. In all cases, the fixed fundamental resonant frequency was between 1.85 GHz to 1.95 GHz. The following subsections show the results obtained. It gives a fair indication of which

methods are best to use in the design process. In all the methods (except chip resistor loading) the bandwidth achieved was very narrow, which is typical of printed antennas. In the case of the chip resistor loading highest percentage size reduction and antenna bandwidth was achieved. Lowest size reduction was obtained with the patch meandering method. One particular observation of interest is that the reduced size of the antenna is a compromise between its bandwidth and gain.

2.3.1 **Patch meandering**

The center frequencies of these antennas were 1.9 GHz. From the results in table 2.1, it can be concluded that incorporating slots on the radiating patch is the better method to help reduce the dimensions of a printed antenna. Also note that the rectangular shape gives the most reduction percentage. The bandwidth is very narrow, typical of a resonant antenna. Figure 2.2 shows some typical slotted patches.

	Reduction Methods			
Antenna Shape	*Slits*		*Slots*	
	Size Reduction (%)	Bandwidth (%)	Size Reduction (%)	Bandwidth (%)
Rectangle	3	0.54	76	0.37
Triangle	4.3	0.05	12	0.27
Circle	48	0.05	56	0.52

Table 2.1: Percentage size reduction and bandwidth for the patch meandering methods

2.3.2 **Shorting Pins**

Table 2.2 shows that loading a chip resistor on the planar antenna can reduce the size dramatically. The rectangular antenna loaded with a chip resistor reduced to a size of 25 mm x 18 mm while the triangular antenna reduced to 28 mm x 20 mm. The bandwidth

is also promising than the shorting pin method. The bandwidth achieved with a short pin loaded circular antenna is 2 % while that loaded with a chip resistor is 6.32 %. However, it must be noted that using a chip resistor has some disadvantages associated with it. The resistors introduce ohmic losses, which degrades the radiation. This effect should especially be considered when designing antennas for mobile devices. The ohmic losses produce lots of heat that may be dangerous to the user. The heat produced also decreases the life of the battery in the mobile. Hence, the shorting pin method is preferred here for size reduction over the chip resistor loading method. A typical shorted patch antenna is shown in Figure 2.1. Several bandwidth enhancements techniques are available in literature that can be used with the shorting pin method. Some bandwidth enhancement techniques are discussed in section 2.4. Note that the rectangular shape again gives the highest percentage size reduction in the case of the shorting pin method

	Reduction Methods			
Antenna Shape	*Shorting Pin*		*Chip Resistor Loading*	
	Size Reduction (%)	Bandwidth (%)	Size Reduction (%)	Bandwidth (%)
Rectangle	76	0.31	81	3.43
Triangle	72	1.59	93	10.31
Circle	48	2.00	92	6.32

Table 2.2: Percentage size reduction and bandwidth for the shorting pin methods

2.3.3 **Material**

Table 2.3 shows that the slow wave structure (SWS) method results in a greater size reduction than using high dielectric constant material. The rectangular shape has the best performance in terms of size and bandwidth. The SWS implementation, however, is

very complex and the design parameters cannot be varied easily. On the other hand, the design procedure for the high dielectric constant material is quite simple. However, surface waves produced in high dielectric materials degrade the radiation pattern greatly. This is usually not preferred because this antenna will not be able to transmit or receive properly as desired. Figure 2.4 shows a typical Slow Wave Structure.

	Reduction Methods			
	High Dielectric Constant		*Slow wave Structure*	
Antenna Shape	Size Reduction (%)	Bandwidth (%)	Size Reduction (%)	Bandwidth (%)
Rectangle	65	0.53	69	1.05
Triangle	33	0.05	76	0.77
Circle	75	1.57	48	0.52

Table 2.3: Percentage size reduction and bandwidth for the High dielectric constant material and the SWS method

2.4 Bandwidth Enhancement Techniques

The microstrip radiator has various attractive features like, lightweight, low cost and easy fabrication. However, it suffers from an inherent limitation of narrow bandwidth. In most cases the impedance bandwidth is not wide enough to handle the requirements of modern wireless communications system. The present day bandwidth requirement is usually greater than or about 10 %. There is an intense amount of literature available on this topic and some of the recent trends in the bandwidth enhancement techniques are discussed briefly in the following paragraphs. Of all the methods discussed below, it will be observed that the common way to increase the bandwidth is to design the antenna to

have dual frequency operation [25,26,27,28]. Also note that all the methods have drawbacks of its own which limits the usage of that particular enhancement method.

A stacked shorted patch is one of the most common ways to increase the impedance bandwidth of microstrip patch antennas. Figure 2.6 shows a typical stacked antenna configuration. If the patches in the stack are made to radiate equally and have a radiation quality factor as low as possible, enhanced impedance bandwidth can be achieved [29]. When two stacked patches are used, two resonant frequencies are obtained. The stacked patches are usually selected to have similar, but unequal dimensions. The substrates between the two stacked patches and between the lower patch and the ground plane can be air, foam or dielectric material. A partial shorting wall or a shorting pin can be used for compact operation [7]. Slots may also be used to further increase the impedance bandwidth. A limitation of this method is that the volume of the antenna increases.

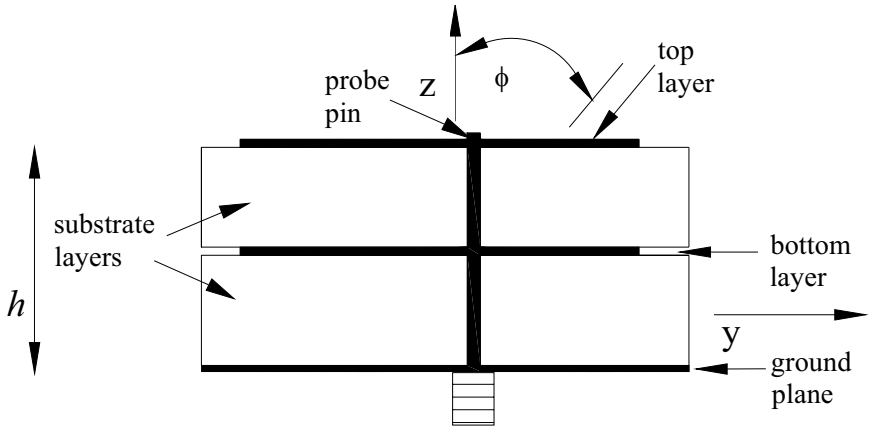

Figure 2.6: A typical stacked printed antenna configuration

A meandered planar inverted – F antenna (PIFA) has been reported to have an impedance bandwidth of 10 times greater than that of a corresponding regular PIFA [30]. The enhanced bandwidth can be achieved by using chip resistor loading, albeit at the cost

of reduced antenna gain. This is due to the ohmic loss of the chip resistor loading. An example of a PIFA is shown in Figure 2.7.

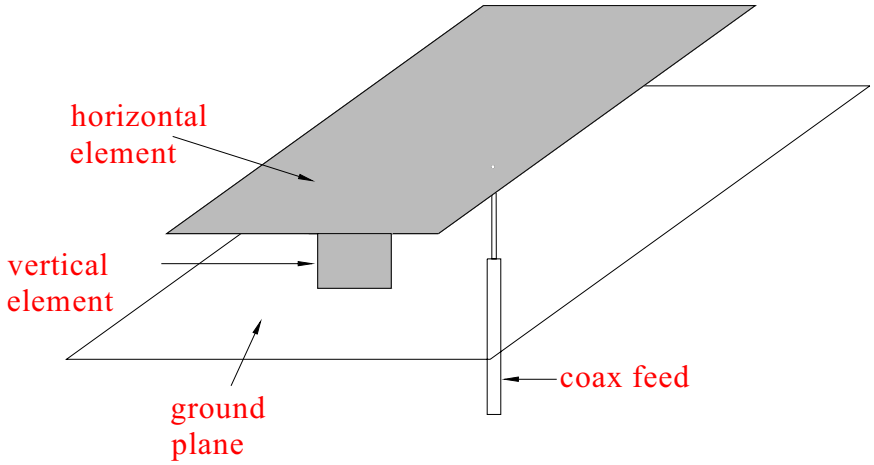

Figure 2.7: Planar Inverted F antenna

Parasitic patches, gap - coupled to the non-radiating edge of the microstrip patch antenna, can also increase the impedance bandwidth [31]. This results because additional resonant modes are closely excited at frequencies near the fundamental frequency of the excited patch. The increase in the total bandwidth has been reported to be 6.35 times more than that of the conventional patch antenna. The parasitic element also adjusts the beamwidth, increases gain and efficiency of the antenna. Another gap-coupled antenna reported in [32] is shown in Figure 2.8. In this paper a bandwidth of 15.4 % was achieved. A drawback with this enhancement method is that the total area of the antenna increases due to the parasitic patches. This is in contrast to the requirements of the mobile communications system antenna. A similar principle is used when antenna arrays are used to enhance the bandwidth. Several resonant frequencies can be generated and with the proper adjustment of the feed pin, a large impedance bandwidth can result.

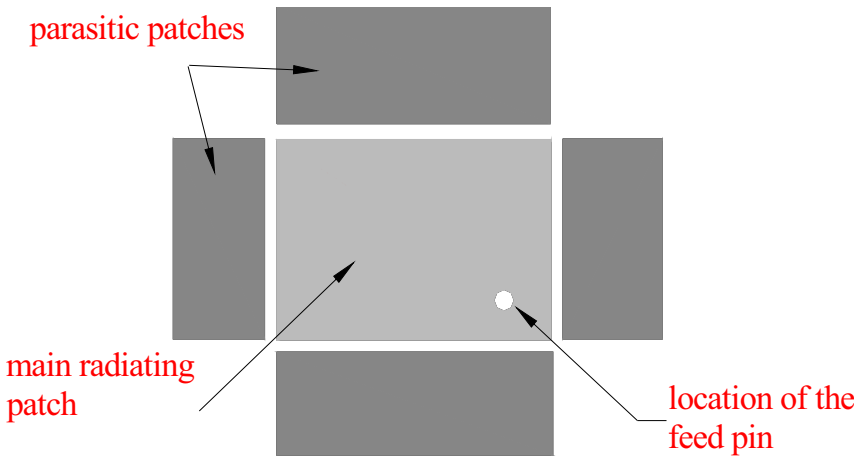

Figure 2.8: Gap coupled microstrip patch antenna

Another area of interest to antenna researchers is the use of frequency selective surface (FSS) to enhance bandwidth. It is created by printing periodic patterns on microwave substrate. Its basic characteristic is to scatter or reflect certain frequencies of electromagnetic waves incident on it. This enables an increase in the passband, which finds significant importance for printed antennas. A broadband design has been developed using this technique [33]. Here multiple layers of FSS are used as part of the substrate. A VSWR (< 2) of 13 % was achieved. The antenna configuration is shown in Figure 2.9.

In order to obtain wider bandwidth, thick foam materials may also be used. A strong coupling is required from the feed line to the patch in this case. A design reported in [34] used *Rohacell* foam of thickness 10 *mm*. The bandwidth achieved in this design was 5.9 %. With a similar note, the substrate thickness can also be increased to increase the bandwidth of compact patch antennas. However, increasing the thickness of the substrate material has disadvantages associated with it. Firstly, a thick substrate

introduces surface waves and hence the radiation pattern is degraded. Secondly, feeding the antenna becomes difficult when a thick substrate is used. Thirdly, higher order cavity mode may be introduced, which will further degrade the radiation patterns [28].

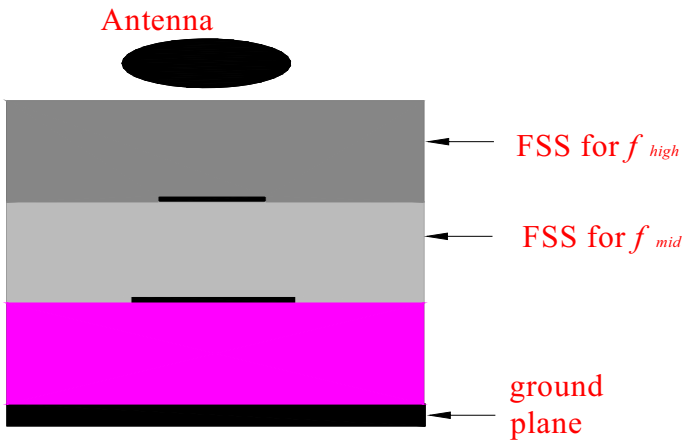

Figure 2.9: A printed antenna on multilayer FSS

Broadband dual frequency operation has also been demonstrated with the use of a V – shaped radiating patch [35]. The V – shaped patch is supported by non-conducting posts and placed above the ground plane of the microstrip feed line, as shown in Figure 2.10. The distance h_1 is small to achieve efficient coupling from the microstrip line to the radiating V – shaped patch. The distance h_2 is much larger to increase the antenna's average substrate thickness and makes possible the excitation of broadband resonant modes. With this configuration, the two impedance bandwidths obtained at the two different frequencies were 20% and 15.6%. The disadvantage with this method is that the volume of the antenna increases and hence it cannot be used for compact antennas. There is also a small dip in the radiation pattern when this method is used.

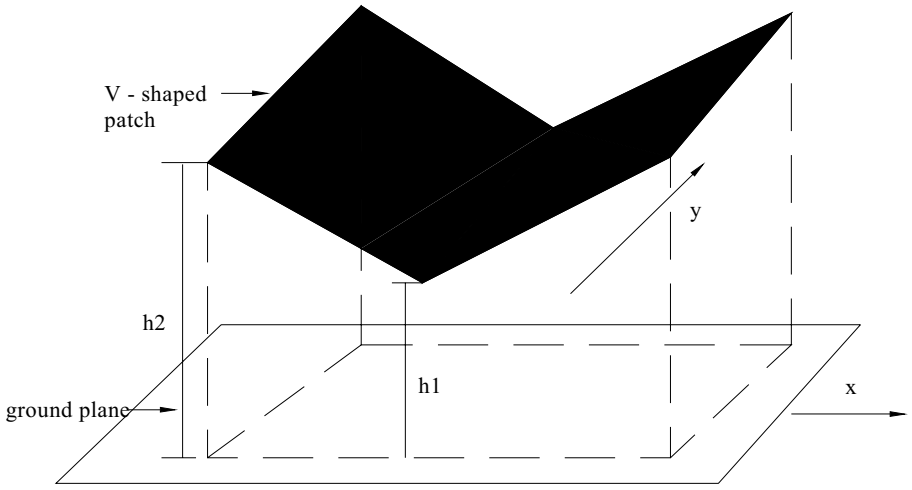

Figure 2.10: Geometry of a broadband dual frequency V – shaped microstrip patch antenna.

Capacitively coupled feed for patch antenna has also been reported for broadband operation [36]. The capacitive feed can have a circular or a rectangular conducting plate to capacitively couple the electromagnetic energy from the source to the shorted radiating patch [7]. With this design, an antenna size of 20 *mm* x 8 *mm* was obtained which had an impedance bandwidth of 9.8 %. This antenna is suitable for DCS cellular communication system.

Loading dielectric resonator on rectangular patch antennas (in suspended microstrip configurations) is used in [37] to increase the bandwidth of the antenna. The optimum position to achieve the maximum bandwidth and best return loss was found to be at the right corner of the radiating edge, away from the feedline. A 10 dB return loss of 13 % can be achieved with this technique.

Several enhancement techniques have been discussed in the above paragraphs. This shows that research into wideband microstrip antennas is still a very relevant topic. In all the designs discussed above, there exists a compromise between the bandwidth, the total

size of the antenna, its gain and its radiation pattern. An optimum solution has to be reached to get the best outcome. Note that most of the designs discussed above have complex design procedures. Of these slots, parasitic elements and stacked configuration will be utilized in this research work for bandwidth enhancement.

2.5 Concluding Remarks

Recent trends in miniaturization of microstrip patch antennas have been discussed in section 2.2. The most common ones include the use of shorting pins, slots and high dielectric constant material. It must be noted that the compact antenna is a result of a compromise between other important features such as impedance bandwidth, gain and efficiency. An optimum solution has to be reached for an optimum performance of the reduced antenna. In section 2.3, analyses of the size reduction technique have been carried out using *Zeland's IE3D EM* simulator. The results depict that the use of shorting pin and slots is the best way forward for miniaturization of patch antennas. It was also noted that in all the methods used (except chip resistor loading), the bandwidth of the antenna was inherently narrow for it to be used in any practical applications. As for the different shapes used for simulation purposes, the rectangular antenna will be the basic form used for easy modification. Section 2.4, therefore, discusses some recent trends to enhance the bandwidth of planar antennas. The analyses carried out in section 2.3 and by using the appropriate bandwidth enhancement techniques outlined in section 2.4, new compact broadband microstrip patch antennas for mobile communications will be designed in this research work.

CHAPTER 3: SMALL DESIGNED ANTENNAS

3.1 Introduction

This chapter presents an in depth design of five compact microstrip patch antennas. The first step is to choose the basic shape of the radiators. Rectangular shaped antennas were chosen since it is simplest to design and fabricate. Its design parameters are also straight forward to revise. Most importantly, from section 2.3, it was found that by incorporating shorting pins and slots on rectangular shaped antennas, a higher reduction in the overall size of the antenna can be achieved. The second step is to choose the type of feeding method to be used. From section 1.1 it was determined to use a coaxial probe feeding technique because of its many advantages over the other feeding methods, such as a robust antenna structure and less spurious radiation from the feed network. The reference antenna is chosen to be a rectangular shaped probe fed microstrip patch antenna operating in the L- and S band of the frequency spectrum. In section 3.2, the configuration and design of a new Y-shaped stacked patch antenna will be discussed. The patches in both the layers are exactly aligned to each other since they have the same geometry. The design uses common size reduction techniques to yield a reduced patch conductor size compared to a conventional rectangular microstrip patch antenna. The proposed antenna is investigated theoretically by means of utilizing a commercial software package. The results of this investigation are discussed in chapter 4.

A novel interleaved F-shaped printed antenna will be presented in section 3.3. Through literature research [38] it was found that a straight F-shaped antenna is a simple

way to reduce the size of a printed antenna. Information is also available in the open literature where inverted F-shaped antennas are used for decreasing the size of patch antennas [38]. In this section, these two F-shaped radiators will be interleaved to obtain size reduction of printed antennas. The inverted F-shape is gap coupled to the straight F-shaped patch. Shorting pins are utilized to further reduce the conductor size.

A third design is presented in section 3.4. It has an interleaved F-shaped antenna as the top radiator and a cross-shaped print [6] for the bottom layer. Foam materials and parasitic rings are used to enhance the total impedance bandwidth of this configuration. Two shorting pins are also used to reduce the size of the antenna. The new antenna configuration and it degrees of freedom will be presented in this section

In section 3.5, a stacked configuration comprising of a square-shaped top radiator and a cross-shaped bottom radiator will be discussed. The square shape has semi circular grooves to reduce its size from a conventional square microstrip patch antenna. Shorting pin is also loaded near the centre of the patch to reduce the overall dimensions. This antenna is easy to fabricate.

Finally, a stacked Y-shaped and an interleaved F-shaped printed antenna will be presented in section 3.6. The basic idea for this design is derived from sections 3.2 and 3.3. Two shorting pins are utilized to help reduce the antenna dimensions while the stacked configuration helps to increase the impedance bandwidth. A bandwidth greater than the bandwidth obtained in section 3.3 have been achieved.

3.2 Y-shaped stacked patch antenna

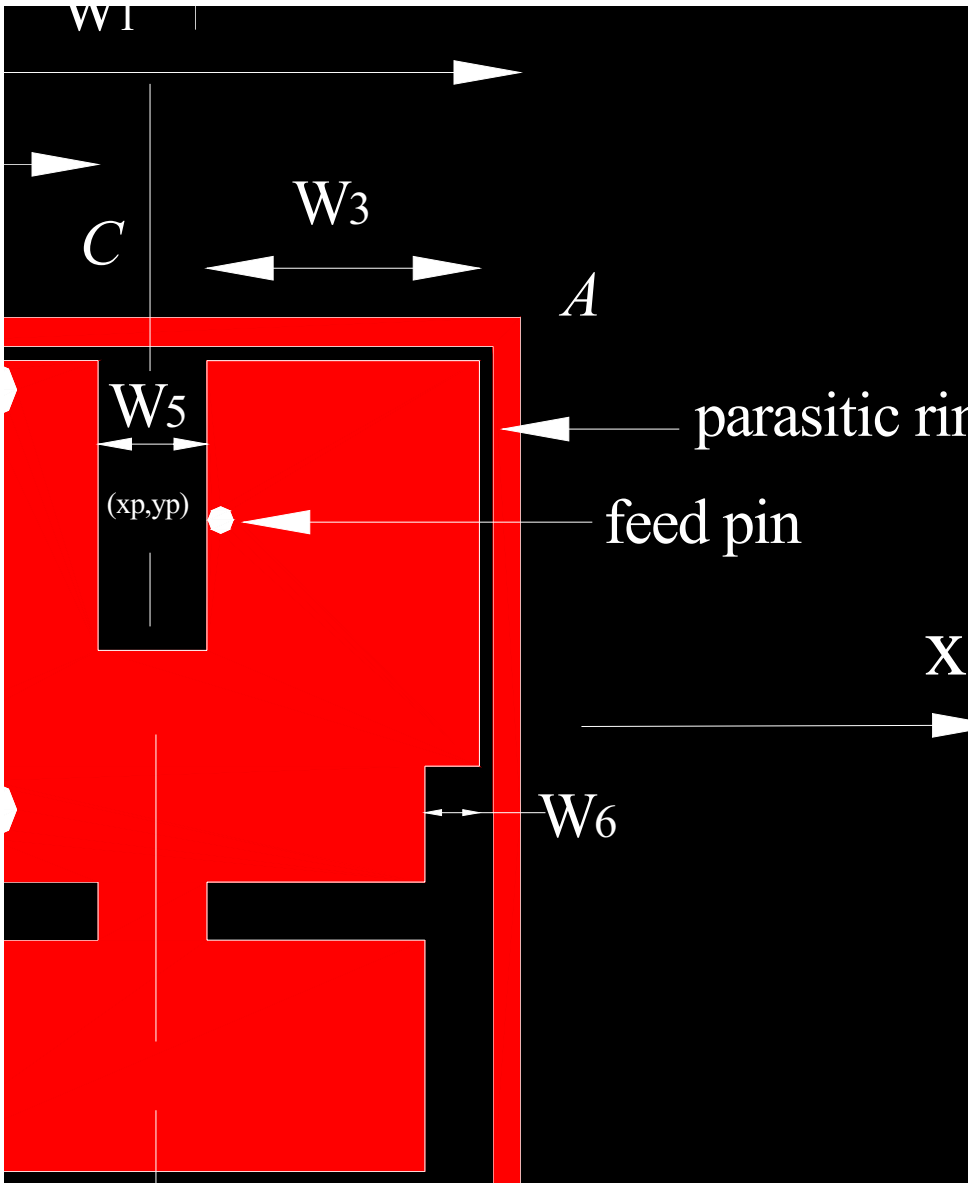

Figure 3.1 Schematic of Y shaped stacked antenna: (a) Top view; (b) Side view

A new Y-shaped stacked patch antenna is presented in this section. This design uses shorting pins, slots and a shorting wall to further reduce the size of a conventional probe fed rectangular patch antenna.

3.2.1 Configuration and Design Strategy

To simulate the design, *Zeland's EM 3D* simulation package, version 11.06 was utilized. Figure 3.1 shows the configuration of the proposed stacked Y-shaped antenna. *Rogers TMM4* ($\varepsilon_r = 4.5, d = 1.27$ mm) is used for the dielectric material. There are two patch layers to this antenna. The top view of the antenna shows a Y-shaped patch. This shape resulted from loading slots on a rectangular patch to reduce its dimensions. The shape is symmetrical about its centerline, *C.* Hence there are two sides to the proposed antenna. On the right of the centerline the probe pin, labeled (xp, yp), is located while on the left side of the centerline, 2 shorting pins of radius r_{sp} are located. The radius of the probe pin is 0.5 mm. A parasitic ring encloses the Y shape. Note that the shape of the bottom trace layer is the same as that of the top trace layer. The 2 dielectric materials used for etching the antenna are separated by *Rohacell* foam of thickness 3 mm. A 3 mm thick foam material also separates the bottom layer and the ground plane. As can be seen from the side view of the antenna, a metallic (shorted) wall at the bottom end of the patch connects the two trace layers.

The explanation of the effects of shorting pins, shorting wall, parasitic ring, foam material and using the same shape in both the trace layers is as follows. As was shown in [7,13] inductive loading such as shorting pin and shorting wall causes the meandering of the surface current which leads to a lengthened current path for a fixed patch linear dimensions. Consequently the fundamental frequency is lowered and a size reduction can be obtained. This technique can be applied to a patch with any shape. If two or more shorting pins are used then the antenna is operated as a quarter wavelength antenna, as in this design. This is another reason why size reduction is observed. Note that size

reduction is achieved albeit at the cost of reduced impedance bandwidth. The design parameters in this design for improving the impedance bandwidth are - the parasitic ring, foam material and the stacked configuration. As was shown in [29] if two stacked patches radiate as equally as possible, the impedance bandwidth can be increased greatly. For the proposed Y-shaped stacked antenna in this research, the patches have the same shape. This is so that they radiate at almost similar frequencies for mutual coupling to occur. In [39] it was shown that by utilizing parasitic elements, the antenna bandwidth, its beam width, gain and efficiency could be adjusted. The parasitic element creates resonance near the main resonance. A similar effect can also be obtained with a parasitic ring around the main radiating patch. While the main patch radiates, the parasitic ring will also radiate around the same frequency. Hence a larger bandwidth can be obtained. Use of thick foam materials with very low dielectric constant again increases the total bandwidth of a microstrip patch antenna as reported in [12].

As can be seen from Figure 3.1 there are many degrees of freedom in the design of this new antenna. The variables are the radius and position of the two shorting pins, position of the probe pin, width of the parasitic ring, the width W_5 ($0.025\lambda_{fr}$), where λ_{fr} is the wavelength at the resonant frequency, and the shorting wall. Radius of the probe pin plays a key role in terms of the antenna characteristics. If the probe pin radius is more than $0.0063\lambda_{fr}$, the return loss of the antenna deteriorates. If the radius is set less than $0.0063\lambda_{fr}$, the resonant frequency decreases together with the bandwidth. If the position of shorting pin 1 is moved towards the center of the patch, the impedance bandwidth decreases. Maximum bandwidth is achieved when shorting pin 1 is placed on the edge of the main radiating patch [40]. When the shorting pin is placed on the edge, an extra

capacitance is created to counter the inductive effect of the patch below the resonance and hence the conductor size reduces. If shorting pin 2 is moved towards the center of the main radiating patch, the impedance bandwidth again decreases. The shorting pins with radius less than 1 mm showed two resonant frequencies, one below the fundamental frequency and one above the fundamental frequency. The higher resonant frequency had a larger bandwidth than the lower resonant frequency. With the absence of one shorting pin, the resonant frequency increased by a factor of 1.61. On the other hand if the width of the parasitic ring is increased, the resonance frequency decreases. Hence the antenna dimensions of the patch can be reduced, albeit at the cost of reduced antenna bandwidth. Therefore, a compromise must be made between the maximum size reduction and the antenna bandwidth achievable. The effect of reducing the dimension W_5 is similar to when the width of the parasitic ring is increased. The fundamental frequency decreases with a decrease in the antenna bandwidth as well. The shorting wall plays a key role in terms of the impedance bandwidth of the antenna. In the absence of the shorting wall, the impedance bandwidth decreases. The simulation results for the configuration in Figure 3.1 will be discussed in section 4.2. The overall size of the configuration shown in Figure 3.1 is L_1 = 31 mm and W_1 = 27 mm. The height of the proposed antenna is 8.54 mm.

3.3 Interleaved F-shaped microstrip patch antenna

There are many antenna configurations where the shape of the conducting patch is meandered to help reduce the size of the overall patch antenna. Some of these include the 'H' shaped antenna [42], the 'C' shaped antenna [43] and the 'E' shaped antenna [44]. A meandered straight F-shaped wire antenna was designed in [38]. Here miniaturized

printed circuit board wire antennas were investigated for WLAN and bluetooth applications. A 57 % reduction in the total area was observed compared to that of an inverted F antenna. In this investigation, a straight F-shaped antenna and an inverted F antenna are interleaved to reduce the overall area occupied by the microstrip patch antenna instead of a wire antenna. The designed resonant frequency, f_r, is 1.9 GHz. The antenna dimension is $0.173\lambda_o$ x $0.1875\lambda_o$ x $0.047\lambda_o$ (where λ_o is the free space wavelength of the antenna) and therefore is suitable for mobile communication applications.

3.3.1 Configuration

Figure 3.2 shows the schematic diagram of the top view and the side view of the proposed antenna. The configuration has an overall length, L_1 = 30 mm and width, W_1 = 28 mm and height, h = 7.27 mm. As mentioned before, the proposed linear polarized printed antenna utilizes the technique of an F-shaped patch conductor to reduce the size of a conventional probe fed microstrip patch antenna. The concept of this antenna is based upon the principal of any dual resonance antenna, namely, that if a mutual resonance can be formed; the overall impedance variation of the antennas will be minimized enhancing the impedance bandwidth of the shorted patches [45].

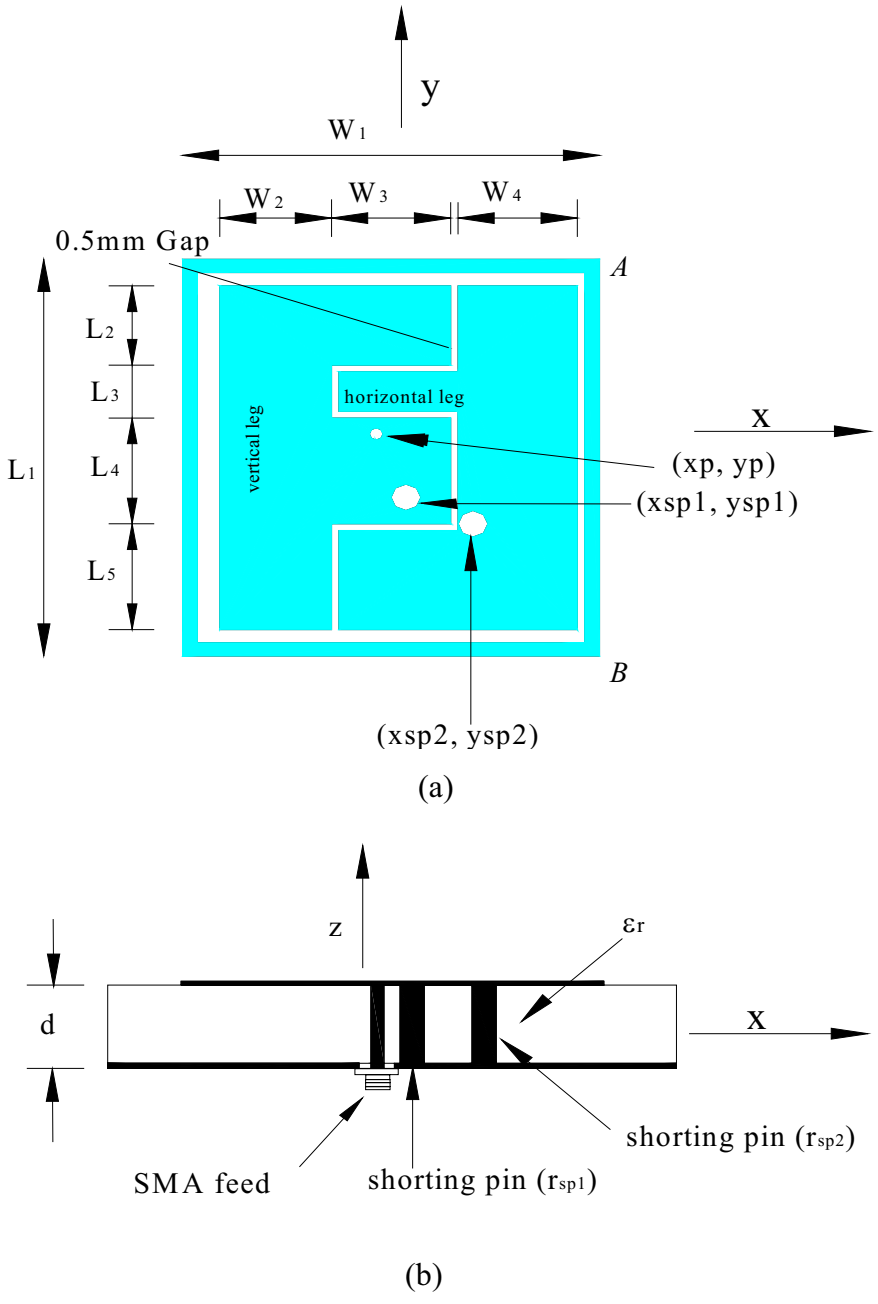

Figure 3.2 Interleaved F- shaped antenna: (a) top view and (b) side view

The antenna consists of two patches, namely, an F-shaped fed patch and an electromagnetically coupled inverted F-shaped patch. In a typical F-shaped printed antenna, there are two regions where radiation takes place. This is the horizontal leg and the vertical leg of the F-shape as shown in Figure 3.2 a. The bandwidth obtained with

only one radiator patch is very small to be used for practical applications such as in mobile communications.

To enhance its bandwidth, an inverted F-shaped patch is coupled to the main radiating patch. This acts as the parasitic patch and radiates mainly due to the horizontal leg. Due to the mutual coupling between the radiators, the impedance bandwidth is improved. The parasitic ring around the main patch also contributes to the total radiation of the antenna. The traditional method of embedding shorting pins in close proximity to the radiating edges of the F-shaped antenna is used here. It is interesting to note that when the shorting pin is removed from the inverted patch, the resonant frequency increases by $0.85\lambda_{fr}$. Large conductor size reduction is achieved in this proposed configuration by maximizing the current path on each printed conductor. To couple power into the antenna, the straight F-shaped patch was connected by a probe feed. This is done here by connecting conducting pins through the dielectric material from the ground plane onto the antenna port labeled (xp, yp). The interleaved F-shaped antennas were designed for an input impedance of $50\,\Omega$. As can be seen from the side view of the antenna schematic in Figure 3.2 b, a thin layer of *Rogers* TMM 4 ($\varepsilon_r = 4.5, d = 1.27$ mm) was used to etch the patches. A *Rohacell* foam layer ($\varepsilon_r = 1.07, d = 6$ mm) is sandwiched between the two dielectric layers.

Through simulations it was found that three variables are important with respect to the bandwidth of the antenna and its size. These variables are the horizontal and vertical legs of the F-shape and the position of the probe pin (refer to Figure 3.2 (a)). When the horizontal leg of the straight F shape is decreased, the bandwidth decreases at the expense of reduced antenna size. The bandwidth obtained was 7 %. This is a still

considered small in terms of its bandwidth. However when the vertical leg is made smaller, the bandwidth decreased dramatically to 2.9 %, again with the advantage of a smaller patch size. This shows that the vertical leg affects the radiation of the antenna to a greater extend than the horizontal leg. These two simulations also show that both the legs of the F shape are important radiators. Meanwhile when the horizontal leg of the inverted F shape is decreased, a 2 % increase in the total impedance bandwidth is obtained. However, the resonant frequency also increases. Therefore a compromise must be reached between the desired bandwidth and the required resonant frequency. With a decrease in the vertical leg, the bandwidth decreases slightly while resonating at the same fundamental frequency. These show that the inverted F shape is not dependent on its vertical arm for radiation. The antenna is manufactured and tested. The experimental and simulation results are discussed in chapter 4.

3.4 Stacked Antenna: Interleaved F- shaped and Cross-shaped patch

The configuration discussed in section 3.3 may be utilized in a stacked configuration. The F-shaped patch is used for the top layer and a cross - shaped [6] patch is utilized for the bottom layer. This is so since the cross shape enables more reduction due to lengthening of the current path. In this section a novel interleaved F-shaped antenna is presented in a stacked configuration where the bottom layer is a cross-shaped conductor.

3.4.1 Configuration and Design Strategy

Figure 3.3 shows the configuration of the proposed antenna. The substrate material used is *Rogers* TMM4 ($\varepsilon_r = 4.5, d = 1.27$ mm). This antenna was designed for

operation at 1.9 GHz. As mentioned before to achieve larger bandwidth a stacked configuration is used. The top layer, as mentioned previously, has an interleaved F-shaped patch. There are two F-shapes electromagnetically coupled by a 0.5 *mm* gap. The right side up F-shape patch contains the coaxial probe pin of radius, $r_{p,}$ labeled (xp, yp) and a shorting pin of radius, r_s, labeled (xsp1, ysp1). A shorting pin, labeled (xsp2, ysp2), is also incorporated on the inverted F-shape such that the resonance produced is near the desired resonance of 1.9 GHz. This structure is based on the work of [46] where the bandwidth of the antenna is increased by closely spacing parasitic patches on the same layer as the fed patch. The bandwidth obtained with a single F-shape is not sufficient for practical applications. For further bandwidth improvement, a parasitic ring is placed around the main radiating element.

The bottom trace layer is cross-shaped and surrounded by a parasitic ring as well. Research [6] has shown that cross – shaped patch is a good technique to reduce the size of a patch antenna. This is so since the current path is lengthened in this configuration (Figure 3.3 c). The presence of this layer enables a third resonance. With proper alignment of the shorting pins and the probe pin, all the 3 resonance's can be merged together to form an antenna with a good impedance bandwidth. Similar to the Y-shaped antenna, the 2 dielectric layers are separated by *Rohacell* foam ($\varepsilon_r = 1.07, h = 3\,\text{mm}$). Note that the shorting pin from the inverted F-shape has no effect on the bottom trace layer since it does not penetrate through the conducting element. Basically this bottom layer has a feed pin and one shorting pin, from the top patch, extending to the ground plane. The total thickness of this antenna configuration, *h,* is 8.54 mm with an overall dimension of 30 mm *(*L_1*)* x 28 mm *(*W_1*)*.

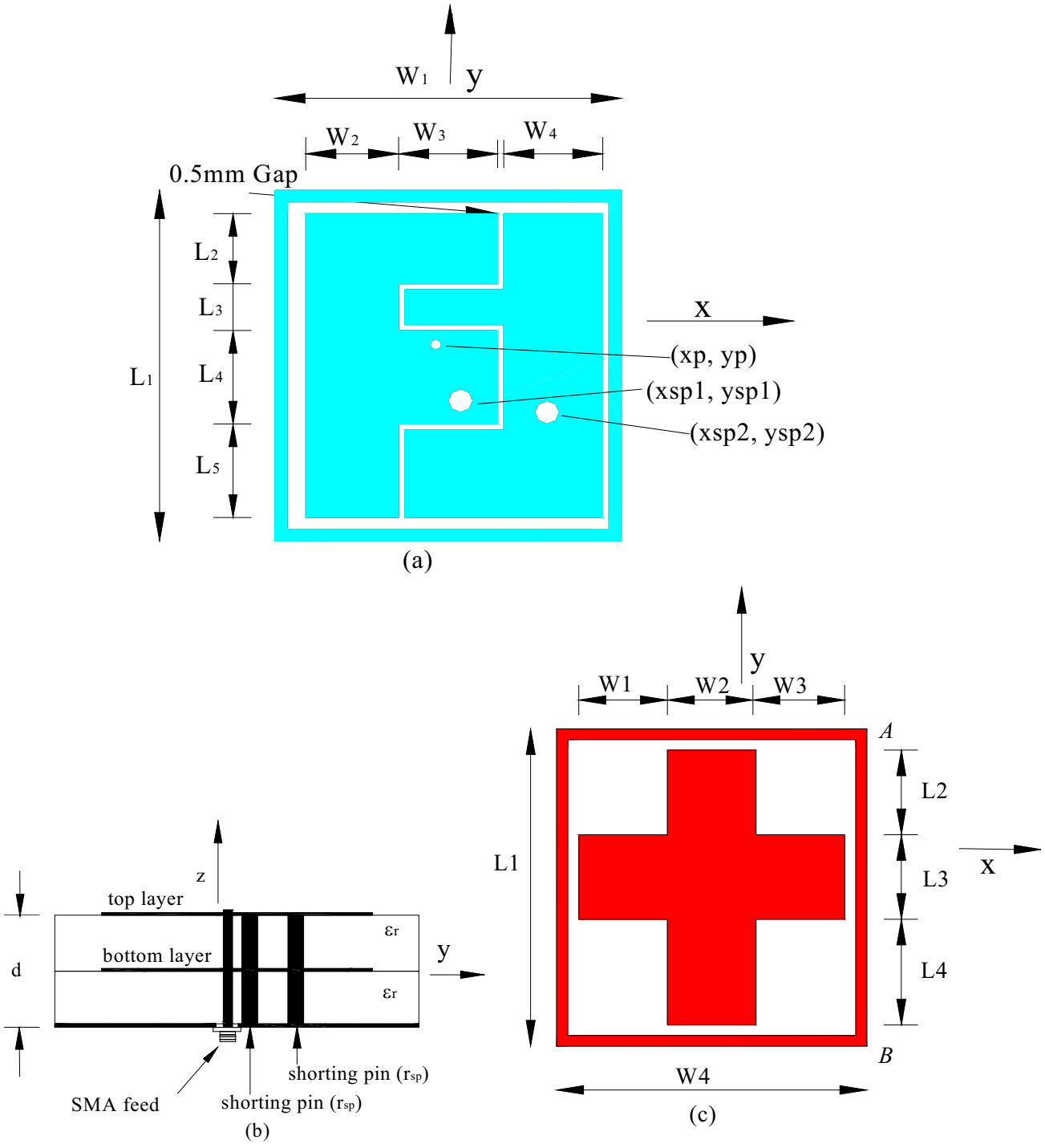

Figure 3.3 Schematic of the interleaved F- shaped + cross- shaped antenna: (a) top trace layer, (b) side view and (c) bottom trace layer.

The degrees of freedom associated with this antenna with respect to the top radiating layer are as follows: position of the shorting pin and the probe pin, radius of the shorting pin and the probe pin and the parasitic ring. Through simulations it was found that if the positions of the shorting pins are moved towards the outer edges, the resonant frequency shifts from 1.85 GHz to 2.2 GHz. When the probe pin is moved towards the shorting pin on the fed patch, the bandwidth is decreased by 6 %. However the resonant frequency also decreased showing that the overall dimension decreased, albeit at the cost of reduced bandwidth. Note that three resonances are obtained around the fundamental resonant frequency when the shorting pin radius, $r_{s,}$ is set less than $0.00625\lambda_{fr}$.

When the radius of the shorting pins are set more than $0.00625\lambda_{fr}$, the bandwidth decreased by 4.27 %. Similar results were obtained when the feed pin radius was set more than $0.003125\lambda_{fr}$. The bandwidth decreases while still resonating at the fundamental frequency. However there is no significant change in the overall bandwidth when the radius of the feed pin increased from $0.003125\lambda_{fr}$ to $0.006333\lambda_{fr}$. Another degree of freedom as mentioned above is the parasitic ring. Positive results were obtained through simulations when the width of the ring was increased. The bandwidth increased by a factor of two with good return loss characteristics. However, this antenna has an enlarged overall size than the original antenna. As expected, with the removal of the parasitic ring from the top patch layer, the impedance bandwidth slightly decreases.

The bottom layer variables are due to the antenna shape and the parasitic ring. With an increase in the overall copper area, the bandwidth decreased by 1.9 %, whilst resonating at the same fundamental frequency. The increased copper content also improves the linear radiation. If the bottom layer is designed without the parasitic ring,

the bandwidth decreases as expected. Note that as the position and radius of the shorting pin and the probe pin is altered on the top layer, the position and radius of the shorting pin and the probe on the bottom layer is changed simultaneously because of the stacked configuration. Hence it is interesting to note that the effects of changing these parameters would be the same.

Through the above strategies, we found out that by changing the design variables, the antenna characteristics are compromised. These include the overall dimensions, the total impendence bandwidth, the return loss characteristics and the radiation patterns. Therefore these design variables has to be properly selected for the best performance. The geometry in Figure 3.3 was simulated with *Zelands' IE3D* simulation package. The simulation results of the antenna are given in section 4.3.

3.5 Stacked Antenna: Square and Cross – shaped patch

In this section, two shorted patches are presented in a stacked configuration that significantly decreases the resonant frequency of the printed antenna. The antenna utilizes the semi circular grooves technique used in [47] to decrease the size of square printed antennas. Here the semi circular grooves force the current to follow extra semi circular patch. This effectively lowers the resonant frequency of the modified square patch in the S band. This technique can also be applied to a stacked antenna configuration, where one of the patches is a square patch. The second patch layer is a cross-shaped conductor. The obtained antenna is 3 times smaller than a conventional probe fed microstrip patch antenna. This antenna is investigated theoretically with its return loss and radiation characteristics given in chapter 4.

3.5.1 Configuration

Figure 3.4 shows the schematic diagram of the new proposed stacked patch. The antenna is mounted on a grounded substrate of *Rogers TMM 4 ($\varepsilon_r = 4.5, d = 1.27$ mm)*. The total thickness of the antenna is h = 8.54 mm. The overall size of the antenna is L_1 = 30 mm x W_1 = 28 mm. The upper trace layer is a square patch with a parasitic ring of width W_4. To couple power coaxial probe of radius, r_p, is located at (xp, yp). Note that both the patches are symmetrical about its centerline, *C*. The antenna also has a shorting pin of radius, r_{sp}, where its centre point is located at a distance of W_3 from the centre of the patch. This shorting pin is almost at the centre of the printed conductor and in close proximity with the feed to reduce the overall size of the antenna [12]. The main objective here is to decrease the overall size of the printed antenna. Apart from the shorting pin, the four semi circular grooves on the main square patch of the top layer maximize the current path length for this purpose. The cross-shaped patch on the second layer produces another resonance due to mutual coupling such that the bandwidth of the antenna improves. This is typical of stacked microstrip patch antennas. This shape is chosen in particular because of its meandered configuration, which enables more radiating slots. The bent shapes resulting from a cross, as shown in Figure 3.4 b, maximize the total current path. From [13] it was found that by maximizing the current path, the resonant frequency of patch antenna decreases and therefore size reduction is observed. As can be seen from Figure 3.4, there are several degrees of freedom for this configuration. The proposed configuration has five variables for a fixed antenna area, namely, the radius of the probe pin, the radius of the shorting pin, the width of the parasitic ring (top and bottom layer), the radius of the circular grooves, *r,* and the size of bends in the cross-shaped layer. To

measure the size reduction of the proposed microstrip patch antenna configuration, *Zeland's EM 3D* simulation package was utilized.

Through several simulations, it was found that decreasing the radius of the feed pin, r_p, did not have much effect on the resonant frequency of the antenna. A decrease of 2 % in the total antenna bandwidth was, however, observed. However, when r_p was increased, the resonant frequency of the antenna increased showing that the total size will increase. The bandwidth obtained with this variable was less than 0.5 %. The opposite effect resulted with changes in the variable r_{sp}. This is probably because by increasing the radius of the shorting pin, greater meandering of the surface current is observed. Thus the resonant frequency decreases and a size reduction is observed. If the radius of the shorting pin is small, less lengthening of the current path results and a lesser size reduction is obtained. Probably the most important variables are the semi circular grooves on the top layer and the perpendicular bends in the bottom patch layer. In theory [47] if the radius of the semi circular grooves are increased, the current path increases. Consequently the resonant frequency decreases. However note that by increasing the radius, *r* shown in Fig. 3.4 a, the total conductor area available for radiation decreases as well. This could have negative effects on this antenna in terms of its radiation patterns. Hence a compromise must be reached between the amount of reduction and the radius of the circular grooves. Through simulations it was found out that the best characteristics were obtained when *r* was 2 *mm*.

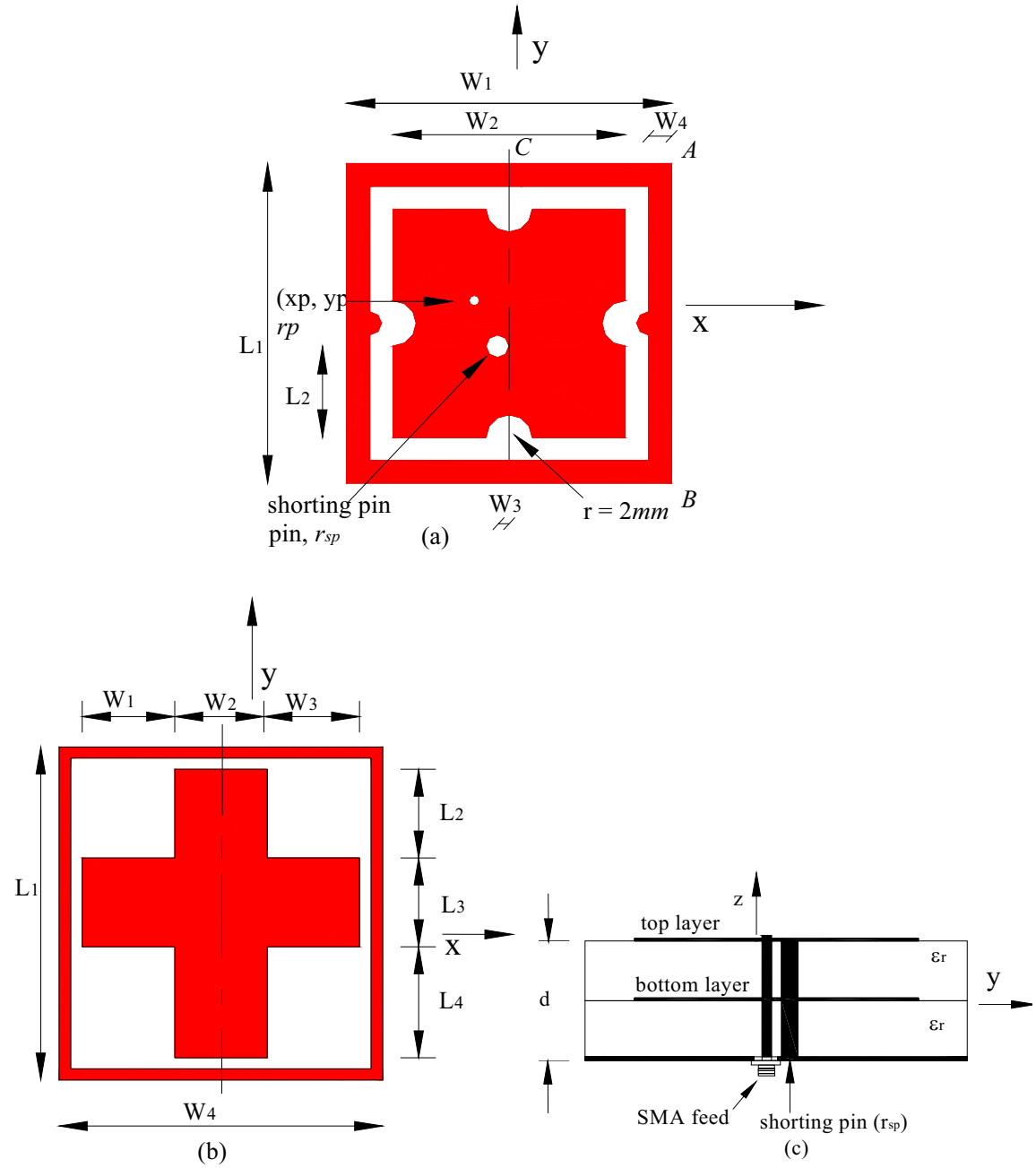

Figure 3.4 Schematic of stacked antenna: (a) square shaped top layer with circular grooves, (b) Cross- shaped bottom layer and (c) side view

When the radius was decreased, there was a decrease in the total antenna bandwidth. The parasitic ring also has a semi circular track protruding towards the main radiating patch. This feature is utilized for the same reason of lengthening the current path. The ring on the other hand enhances the total antenna bandwidth. As discussed in section 3.4.1, when the legs of the cross are made smaller the antenna still resonates at the same fundamental frequency. However, since the length decreases, the bandwidth decreases as well. The effect of changing the radius of the feed pin and the shorting pin is the same as those investigated with the top trace layer.

To test the above-mentioned patch antenna, the geometry in Figure 3.4 was simulated. *Rohacell* foam ($\varepsilon_r = 1.07, d = 3\,\text{mm}$) was sandwiched between the two dielectric layers used for etching the printed antennas and between the bottom dielectric layer and the ground plane. The overall dimensions are W_1 = 28 mm x L_1 = 30 mm. The parasitic ring width for the top layer and the bottom layer was 2 mm and 1 mm respectively. The radius of the feed pin was 0.5 mm while that of the shorting pin was 1 mm. The simulated results will be discussed in section 4.5.

3.6 Stacked Antenna: Y – shaped and F – shaped patch

Two novel Y-shaped and F-shaped antennas were designed in section 3.2 and 3.3 respectively. The bandwidth obtained with the stacked Y-shaped configuration was 2.7 % more than the F-shaped antenna. However, the total volume of the Y-shaped antenna is greater than the F- shaped printed antenna. In this section a method to increase the bandwidth of the F-shaped antenna is proposed whilst maintaining a small size. The configuration uses stacked configuration where the top patch layer is the Y-shaped

printed conductor and the bottom layer is the interleaved F-shaped printed conductor. The total bandwidth is increased with this compact microstrip patch antenna configuration.

3.6.1 Configuration and Design Strategy

If mutual resonance can be formed between these two antennas, then the resonant frequency is expected to increase from that obtained with an interleaved F-shaped antenna in section 3.3. Figure 3.5 shows the proposed configuration. A feed pin, labeled (xp, yp), extends from the ground plane to the top layer to couple power to the antenna. Two shorting pins are loaded to reduce the total antenna dimensions. The first shorting pin, labeled (xsp1, ysp1), is placed at the upper edge of the Y-shaped patch. The upper shorting pin has been moved down by 2 mm to tune the resonant frequency of this proposed configuration. The second shorting pin, labeled (xsp2, ysp2), has been loaded 13 mm in the –y direction from the first shorting pin with the same radius. The second layer, as mentioned previously, is an interleaved F-shaped patch. The two shorting pins, from the top-conducting layer, penetrate through the coaxial probe fed straight F-shaped patch. Note that the two shorting pins do not affect the electromagnetically coupled F-shaped patch on the second layer. *Rogers* TMM 4 with $\varepsilon_r = 4.5$ and thickness 1.27 mm is used to etch the two layers. *Rohacell* foam material of thickness 3 mm and $\varepsilon_r = 1.07$ is sandwiched between the two dielectric materials for bandwidth enhancement. The overall dimension of the patch is L_1 = 31 mm and W_1 = 28 mm.

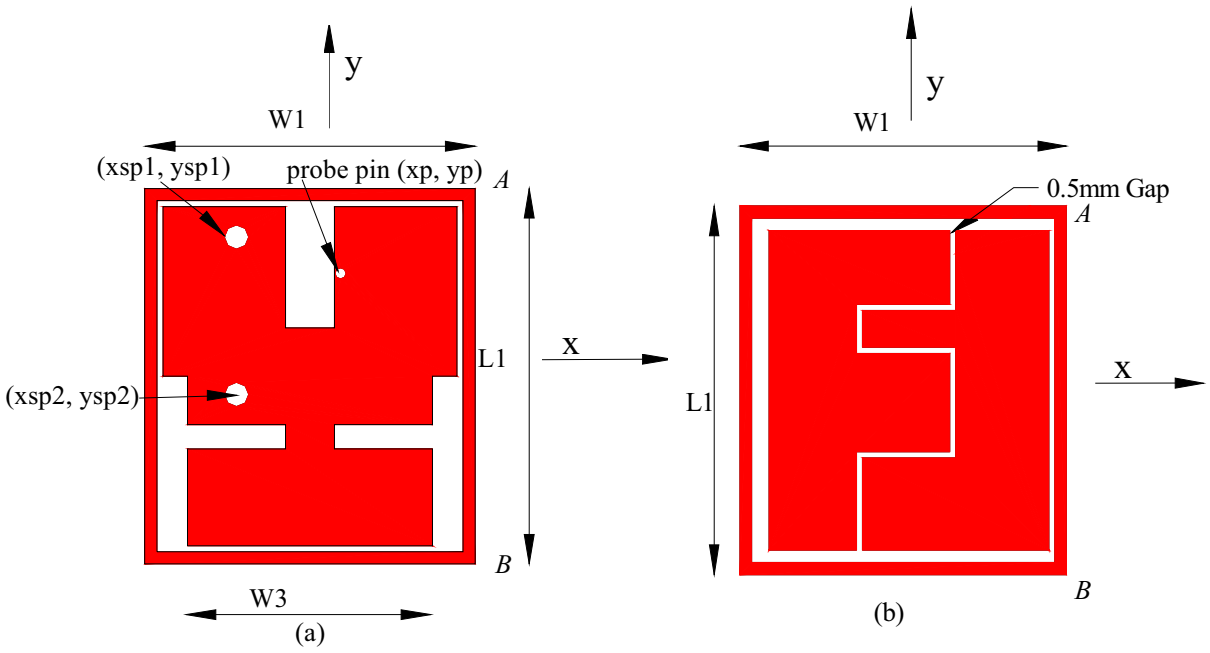

Figure 3.5 Y-shaped and an interleaved F-shaped stacked antenna: (a) top layer (b) bottom layer

The degrees of freedom associated with this proposed configuration are similar to that mentioned in section 3.2 and section 3.3. Through simulations it was found that if the radius of the shorting pins is decreased, the current path decreases and hence the resonant frequency increases. Meanwhile an increase in the width of the parasitic ring has adverse effects on the bandwidth of the printed antenna. The shorting pins, when placed at the edges of the top radiator, showed good return loss characteristics compared to its positions in the center of the patch. With respect to the bottom conductor layer a decrease in the horizontal leg of the straight F resulted in an indefinite decrease in the impedance bandwidth of the antenna, as expected. Similarly, a decrease in the horizontal leg of the inverted F shape reduced the bandwidth of the antenna by 1 % showing that the horizontal leg is used in the radiation of the EM waves. To test the antenna shown in

Figure 3.5, it was simulated using *Zeland's IE3D* simulation package. The results are discussed chapter 4.

3.7 Concluding Remarks

This chapter has presented five new microstrip patch antenna designs that are suitable for mobile communications. For each design, its design variables have been studied to better understand the varying antenna characteristics. It was determined through various simulations that there is always a compromise between the antenna characteristics. For example, a very small antenna has a narrow impedance bandwidth. Therefore the variable has to be chosen appropriately such that the antenna is small and has a reasonable bandwidth as well. All the antenna design has been simulated using the geometry given in the respective sections. These antennas have also been simulated using *Rogers TMM 4* materials. It is interesting to note that the interleaved F-shaped antenna has the smallest volume compared to the other four antennas. The stacked Y-shaped and F-shaped antenna, on the other hand, has the greatest volume. Although the other three antennas discussed in sections 3.2, 3.4 and 3.5 have different geometry, their overall dimensions are the same. Note that all the proposed antennas are small in size such that it can be used for mobile applications.

CHAPTER 4: RESULTS AND DISCUSSION

4.1 Introduction

This chapter will discuss the simulation results for the five proposed antennas. In addition, one antenna, namely the interleaved F-shaped antenna is fabricated and experimentally tested to valid the design of the antenna using the software package. The result of this experiment will be discussed in section 4.7. These results are compared to the simulated results. All simulation of the designed antennas has been carried out using *Zeland's IE3D simulation CAD package.* It must be noted that in the case of a linear polarized antenna, the co - polarization radiation is given by the total radiation (E-total) in the *IE3D Software Package*. The cross – polarization level is given by E-phi [4]. The radiation patterns and return loss characteristics are presented in this chapter for all the designs mentioned in chapter 3.

The simulation results for the Y-shaped stacked antenna are presented in section 4.2. A 10 dB impedance bandwidth is obtained from the simulation results to determine the frequency spectrum of the antenna. The radiation pattern of this antenna is presented here at approximately 1.9 GHz. In section 4.3, the return loss behavior and the radiation pattern of the interleaved F-shaped antenna are presented. This antenna has an electromagnetically coupled F-patch antenna that provided a second resonance resulting in a reasonable bandwidth. Furthermore, the simulation results of an interleaved F-shaped and cross-shaped antenna are discussed in section 4.4. This is a stacked antenna where the top layer is the interleaved F-shaped antenna and the bottom radiating patch is cross-

shaped. The results show that antenna size reduction is achieved. In section 4.5, simulation results of another stacked antenna are presented. The top patch layer is square shaped while a cross-shaped pattern is used for the bottom layer. The return loss behavior and the radiation pattern of the antenna at 1.87 GHz are discussed here. Finally, the simulation results of a stacked antenna with a Y-shaped top layer and an interleaved F-shaped bottom layer are presented in section 4.6. The total impedance bandwidth is determined from the return loss plot. In addition, the radiation plots presents information such as cross – polarization levels and the gain of the antenna.

4.2 Y-shaped stacked patch antenna

Figure 4.1 shows the calculated return loss behavior of the Y-shaped stacked microstrip antenna. This result is achieved by utilizing the designed antenna configuration shown in Figure 3.1. The parameters of this configuration are listed in the figure caption below. As can be seen from Figure 4.1, the simulated result shows that the antenna operates from 1.8 GHz to 2 GHz with a bandwidth of 200 MHz. The 10 dB return loss bandwidth of this proposed antenna configuration is 10.2 %.

This bandwidth is reasonably high utilizing the concept of any dual resonance antenna where it states that if a mutual resonance can be formed; the overall impedance variation of the antenna will be minimized, enhancing the bandwidth of the antenna [45]. The fundamental resonant frequency is approximately 1.9 GHz. It should be noted that without the presence of the shorting wall, the return loss bandwidth of the antenna decreases to 8 %.

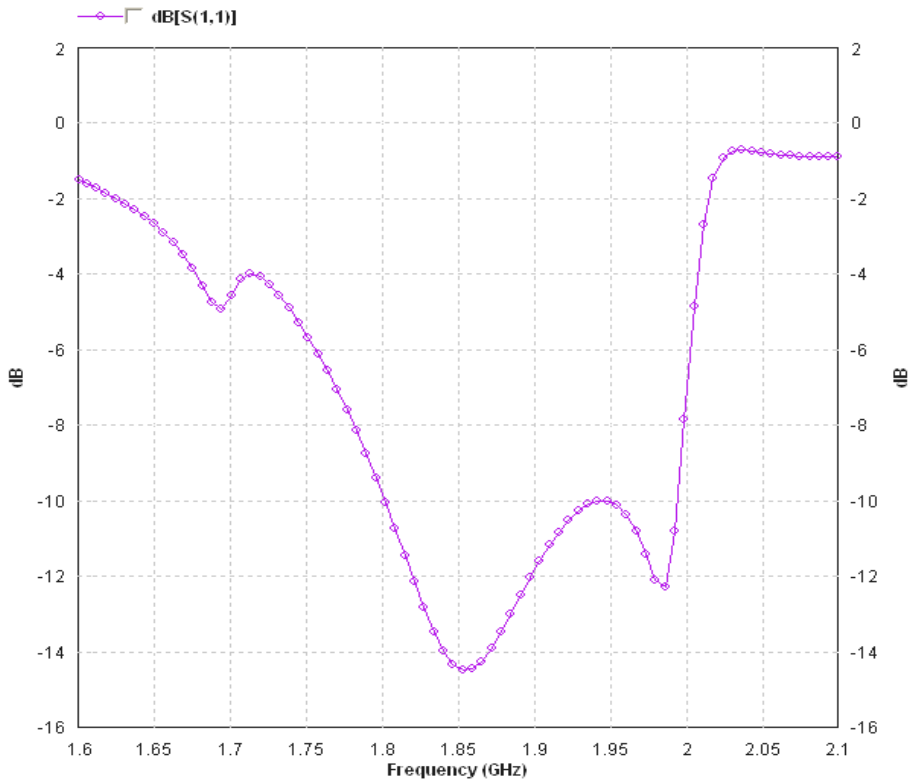

Figure 4.1: Return loss characteristic of the Y-shaped stacked printed antenna

Parameters: $L_1 = 31mm$, $L_2 = 14\ mm$, $L_3 = 8\ mm$, $L_4 = 1.5\ mm$, $W_1 = 27\ mm$, $W_2 = 10\ mm$, $W_3 = 10\ mm$, $W_4 = 5.5\ mm$, $W_5 = 4\ mm$, $W_6 = 2\ mm$, $W_7 = 20\ mm$, xp = 16 *mm*, yp = 24 *mm*, $r_{sp} = 1\ mm$

Since a microstrip patch antenna radiates normal to its patch surface, the elevation pattern for (E-total) $\phi = 0$ and $\phi = 90$ degrees would be important [48]. As stated previously, this antenna is linear polarized. Therefore, the cross – polarization levels can be determined from the E-phi radiation patterns. Figure 4.2 below shows the simulated radiation patterns of the proposed antenna at approximately 1.9 GHz. The ground plane for this measurement was assumed to be infinite for simulation purposes. A small dip can be seen on the broadside. This pattern is similar to a probe fed patch antenna shorted by a shorting strip [7]. Note that in Figure 4.2, the broadside of the antenna is 0°. The radiation patterns are fairly symmetrical about the broadside. The gain of the antenna at the broadside was calculated to be –1.7 dBi. This is expected due to the patch size reduction [49].

To put these results into perspective, a conventional probe-fed rectangular antenna designed to operate at this frequency using the same substrate material has the dimensions of 74 mm x 32 mm. However, the new interleaved F-shaped antenna has an overall conductor area of 31 mm x 27 mm. Thus the new antenna is smaller by a factor of 3 comparing the conductor area. The antenna bandwidth is 9.7% more than a conventional shorted patch antenna. From the results it can be said that this compact antenna can be used for wireless mobile communications operational in the L band frequency range. The overall size of the antenna is $0.19\lambda_o$ x $0.17\lambda_o$ x 0.05 λ_o (λ_o is the wavelength of the antenna in free space). The antenna is small enough to fit into most mobile handsets. The size of Nokia 1100 mobile phone is almost 3 times larger than the size of this new antenna design.

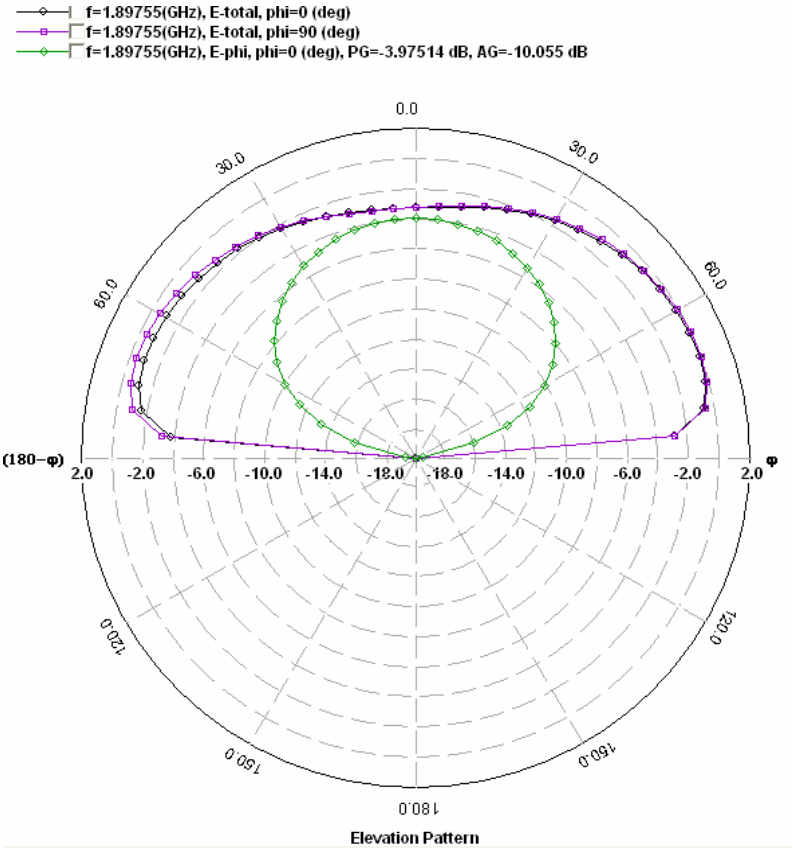

Figure 4.2: Radiation patterns of the Y-shaped stacked antenna

4.3 Interleaved F-shaped microstrip patch antenna

The simulated return loss behavior for the interleaved F-shaped patch antenna is shown in Figure 4.3. The antenna is assumed to be mounted on a thin layer of TMM 4 dielectric material. The dielectric substrate and the ground plane are separated by a 6 mm *Rohacell* foam (refer to Figure 4.3 captions for dimensions). The 10 dB return loss bandwidth of the antenna was 140 MHz, achieving a bandwidth of 7 % at a center frequency of 1.9 GHz. The electromagnetically coupled F-patch antenna provided a second resonance resulting in a reasonable bandwidth. For further verification of results, this antenna was fabricated and tested. Section 4.7 discusses the measured results of the patch antenna.

The radiation pattern of the interleaved F-shaped antenna was calculated using *Zeland's IE3D* simulation package. An infinite ground plane is assumed in this simulation. Figure 4.4 shows the simulated patterns at 1.88 GHz. The cross polarization radiation (E-phi) is significant, which is similar to conventional probe fed rectangular antenna with thick air or foam substrate [50]. The total radiation at $\phi = 0$ degrees is almost omni – directional about the broadside. The total radiation at $\phi = 90$ degrees has a large dip at 135°. The simulated gain of the antenna at this resonant frequency was 1 dBi at the broadside. In terms of its overall patch area, this interleaved antenna is 65 % smaller than a standard probe fed rectangular antenna. Note that the conductor area of a standard probe fed rectangular antenna mounted on the same substrate material is $0.46\lambda_o$ x $0.2\lambda_o$. The conductor area of this new antenna is $0.19\lambda_o$ x $0.18\lambda_o$ with a height of $0.05\lambda_o$. This antenna has a bandwidth that is compliant with systems such as the personal communication service (PCS).

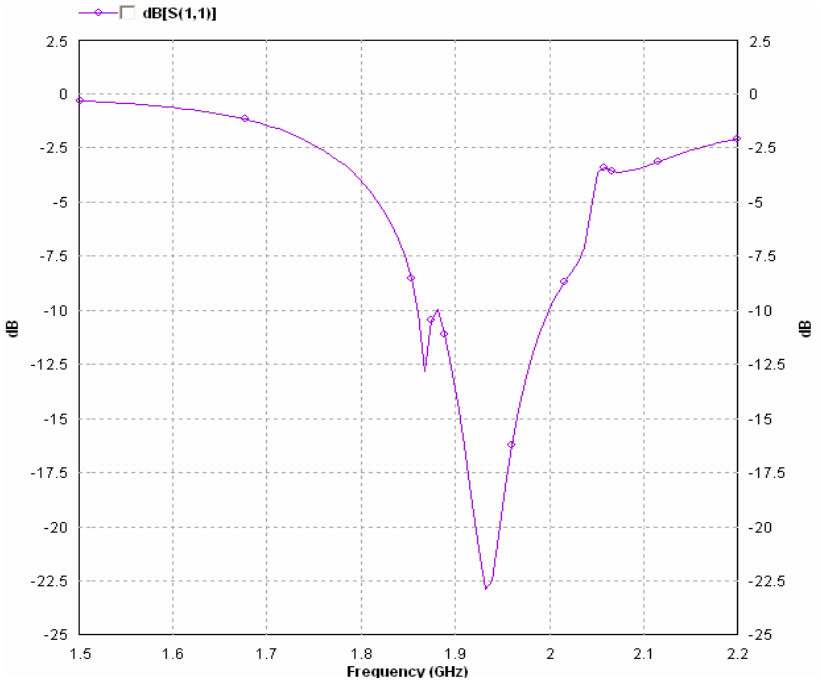

Figure 4.3: Predicted return loss of the interleaved F-shaped antenna

Parameters: xp = 14 *mm*, yp = 16.8 *mm*, xsp1 = 15 *mm*, ysp1 = 12 *mm*, xsp2 = 19.5 *mm*, ysp2 = 10 *mm*, L_2 = 6 *mm*, L_3 = 4 *mm*, L_4 = 8 *mm*, L_5 = 8 *mm*, W_2 = 7.5 *mm*, W_3 = 8 *mm*, W_4 = 8 *mm*, rp = 0.5 *mm*, r_{sp} = 1 *mm*.

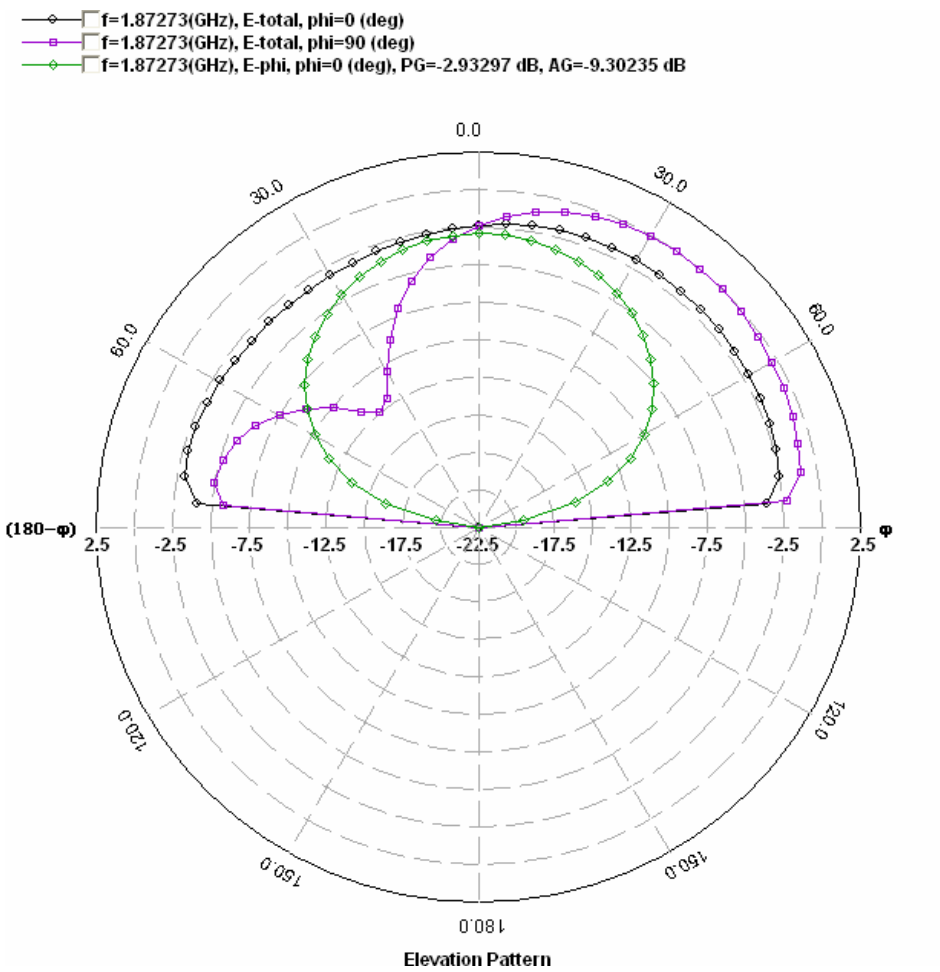

Figure 4.4: Predicted far-field radiation pattern

4.4 Stacked Antenna: Interleaved F-shaped and Cross-shaped patch

Figure 4.5 shows the predicted return loss of the interleaved F-shaped and cross-shaped stacked antenna. The dimensions of the antenna are shown below the figure caption of Figure 4.5. As can be seen from the plot, the impedance bandwidth of the antenna determined from the –10 dB return loss is 10.5 % covering from 1.782 GHz to

1.981GHz. This is more than that of a conventional microstrip patch antenna of 1.9 % [24]. This predicted bandwidth is compliant with systems such as DCS 1800 (1805 MHz-1880 MHz), Digital European Cordless Telephone (1880 MHz-1990 MHz), Personal Handy Phone System (1895 MHz-1918 MHz) and PCS systems. The centre frequency is at 1.86 GHz. The relatively high bandwidth of the antenna is due to the stacked configuration [29], the use of foam materials and the parasitic ring for extra coupling. This new antenna configuration has a conductor area of 30 mm x 28 mm. A traditional rectangular antenna designed with the same substrate material has a total patch area of 74 mm x 32 mm. A 65 % reduction in the overall patch size resulted from using this antenna configuration over the traditional rectangular patch antenna. Although this antenna has a stacked configuration, it is practically easy to manufacture. The antenna has less solder joints and is therefore more robust.

The predicted far- field radiation pattern of the interleaved F-shaped and cross-shaped antenna is plotted in Figure 4.6. The total radiation is almost omni-directional in the plane $\phi = 0$ degrees. Note that the cross-polarization radiation is significant. The radiation pattern at $\phi = 90$ degrees is also shown. In this plane a large dip is seen on the left side of 0°. The ground plane of the antenna is assumed to be infinite for simulation purposes. Note that due to the antenna size reduction, a decrease in the antenna gain is expected [7]. The simulated gain of this configuration was 0.9 dBi.

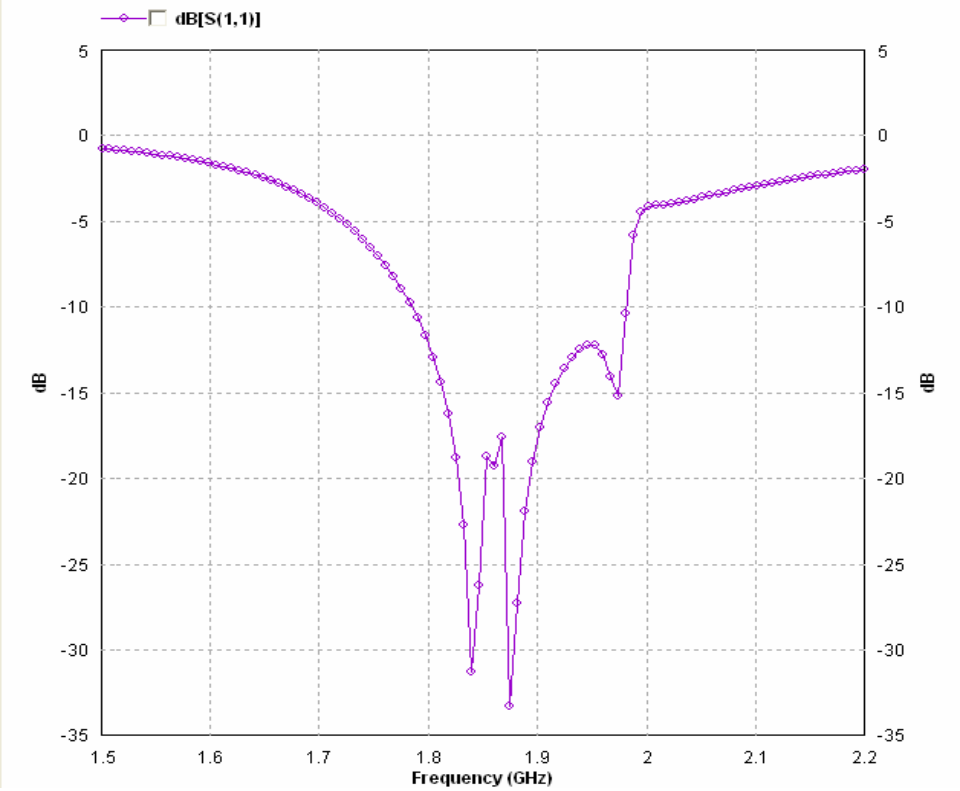

Figure 4.5: Simulated return loss of the F-shaped and the cross-shaped stacked antenna

Parameters: **(a)** xp = 13 *mm*, yp = 16.8 *mm*, xsp1 = 15 *mm*, ysp1= 11.5 *mm*, xsp2 = 22 *mm*, ysp2 = 11 *mm*, L_2 = 6 *mm*, L_3 = 4 *mm*, L_4 = 8 *mm*, L_5 = 8 *mm*, W_2 = 7.5 *mm*, W_3 = 8 *mm*, W_4 = 8 *mm*, r_p = 0.5 *mm*, r_{sp} = 1 *mm*; **(b)** L_1 = 8 *mm*, L_2 = 8 *mm*, L_3 = 10 *mm*, W_1 = 28 *mm*, W_2 = 8 *mm*, W_3 = 8 *mm*, W_4 = 8 *mm*.

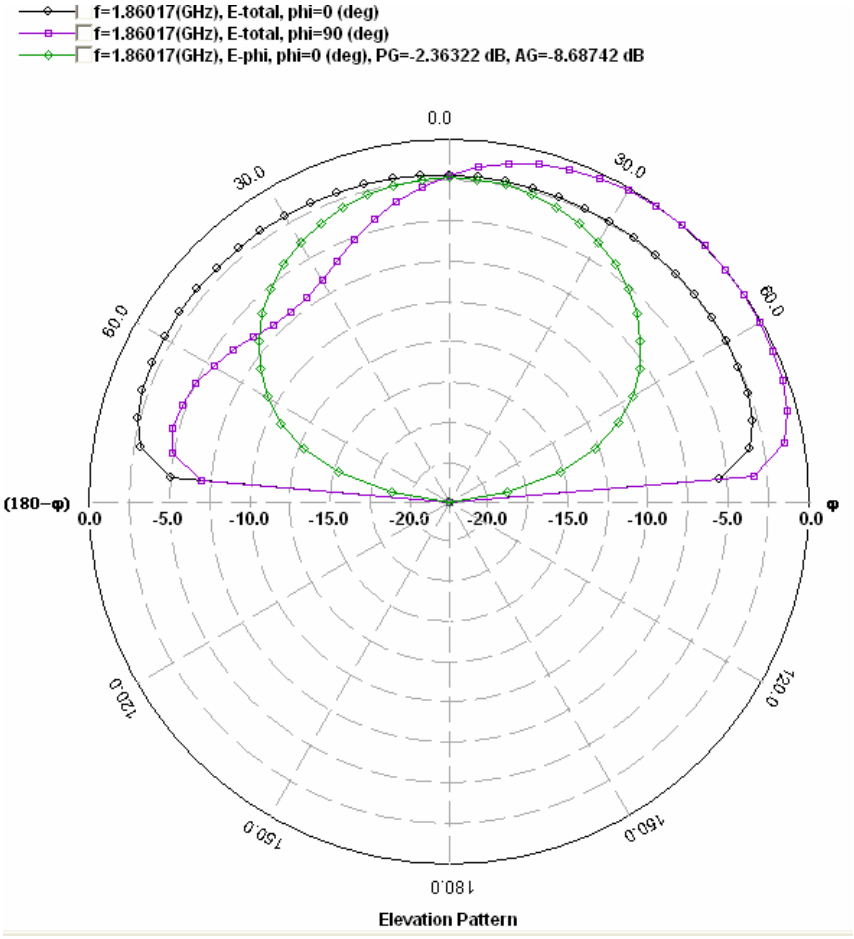

Figure 4.6: Simulated radiation patterns of the interleaved F-shaped and cross-shaped antenna at approximately 1.86 GHz

4.5 Stacked Antenna: Square and Cross-shaped patch

The simulated return loss of the square and cross-shaped stacked antenna is shown in Figure 4.7. The antenna was simulated using the configuration shown in Figure 3.4. The configuration parameters are shown in the figure caption of Figure 4.7. The antenna operates from 1.846 GHz to 2.002 GHz. The 10dB return loss bandwidth (VSWR > 2) is 8.4 %. Conventional patch antennas have a very small bandwidth, typically 1 %. The size of this antenna (L = 30 mm, W = 28 mm) is 65 % smaller than a standard probe fed rectangular printed antenna. This size reduction is due to the use of shorting pins and the semi circular grooves, which lengthens the current path and increases the electrical length of the radiator without increasing the actual size of the radiator. An interesting factor to note is that although the antenna is smaller, the bandwidth has not been compromised due to the two patch layers interacting.

The radiation patterns of this antenna were simulated at 1.87 GHz, and are shown in Figure 4.8. Note that the broadside is at 0°. The co-polarization pattern (E-total) at $\phi = 0$ degrees has similar properties of a conventional printed antenna, that is, the pattern is omni directional. However, the co-polarization pattern at $\phi = 90$ degrees has a higher concentration at the left side of the broadside. Note that the cross-polarization (E-phi) level is high because of the small size of the antenna. Also note that an infinite ground plane is assumed. The simulated gain was obtained to be 0.6 dBi. A method to increase the gain of the antenna is the use of high permittivity superstrate layer [49]. Due to its small size, the antenna can find applications in mobile handsets and other portable devices.

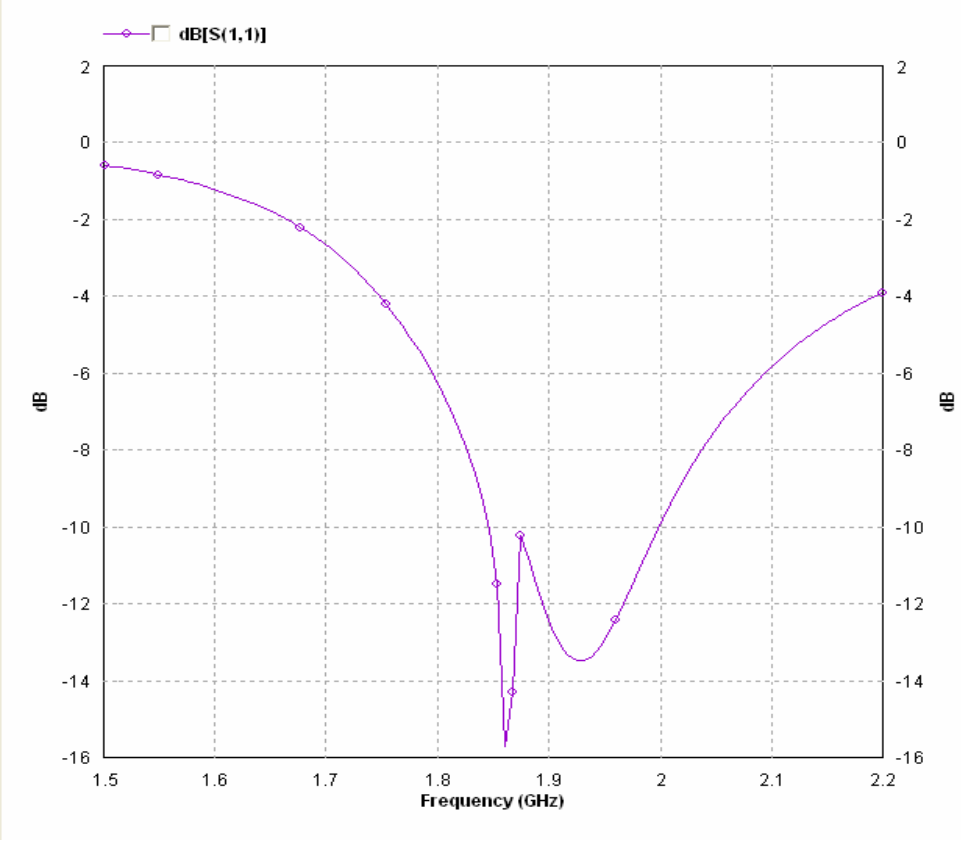

Figure 4.7: Simulated return loss of the square-shaped and cross-shaped stacked antenna

Parameters: **(a)** xp = 11 *mm*, yp = 16 *mm*, xsp = 13 *mm*, ysp = 12 *mm*, r_p = 0.5 *mm*, r_{sp} = 1 *mm*, L_1 = 28 *mm*, L_2 = 8 *mm*, W_1 = 28 *mm*, W_2 = 20 *mm*, W_3 = 0.5 *mm*, W_4 = 2 *mm*; **(b)** L_1 = 8 *mm*, L_2 = 8 *mm*, L_3 = 10 *mm*, W_1 = 28 *mm*, W_2 = 8 *mm*, W_3 = 8 *mm*, W_4 = 8 *mm*.

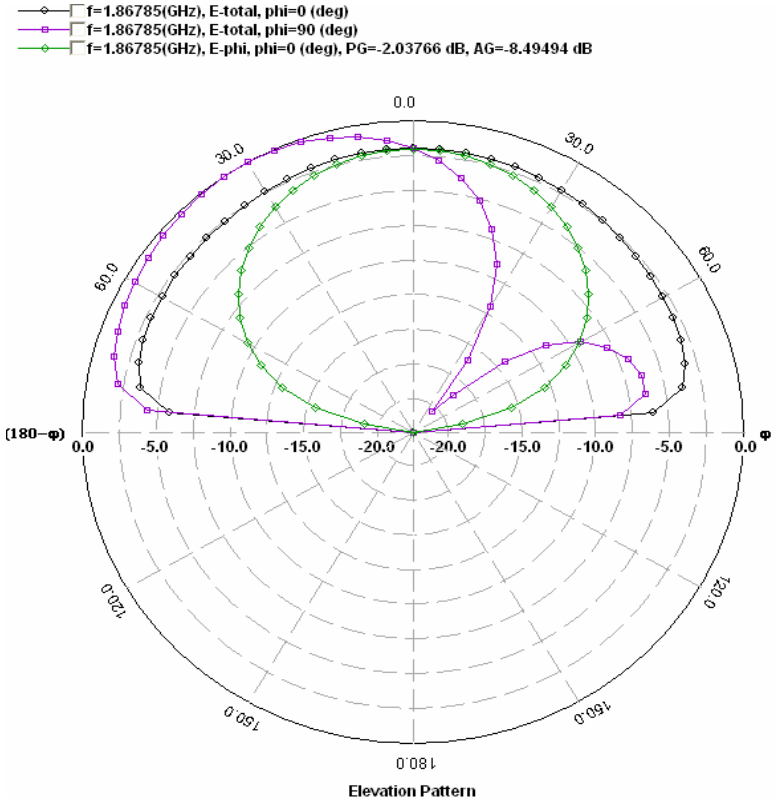

Figure 4.8: Predicted far field radiation pattern of the proposed antenna

4.6 Stacked Antenna: Y-shaped and Interleaved F-shaped patch

Figure 4.9 shows the simulated return loss feature of the Y-shaped and F-shaped stacked antenna. As can be seen from the figure, there are two resonant frequencies operating in the L band. This could be due to the mutual coupling between the inverted and right side up F-antenna in the bottom layer. The first resonant frequency has its centre frequency at 1.61 GHz with a bandwidth of approximately 1%. The second resonance has its centre frequency at 1.87 GHz. The bandwidth here is 8.15%. As stated earlier, the size of a rectangular probe – fed antenna mounted on the same substrate material had an overall patch size of $0.46\lambda_o$ x $0.2\lambda_o$. This new design, however, has a conductor size of $0.19\lambda_o$ x $0.175\lambda_o$. A 63% patch size reduction from the conventional probe fed rectangular patch antenna has been observed. The size reduction is mainly due to the stacked configuration, use of several radiating slots and the use of two shorting pins. The height of this antenna is $0.05\lambda_o$.

Figure 4.10 shows the predicted far – field radiation pattern of the proposed antenna configuration. As can be seen from the figure, a small dip is seen on the broadside and the left side of 0° in both the planes. Note that the broadside is 0°. The pattern is almost omni – directional. This is typical of small patch antennas. The cross – polarization pattern is below the total radiation pattern at the broadside by 1 dB. The gain of this antenna at 1.92 GHz is –0.9 dBi.

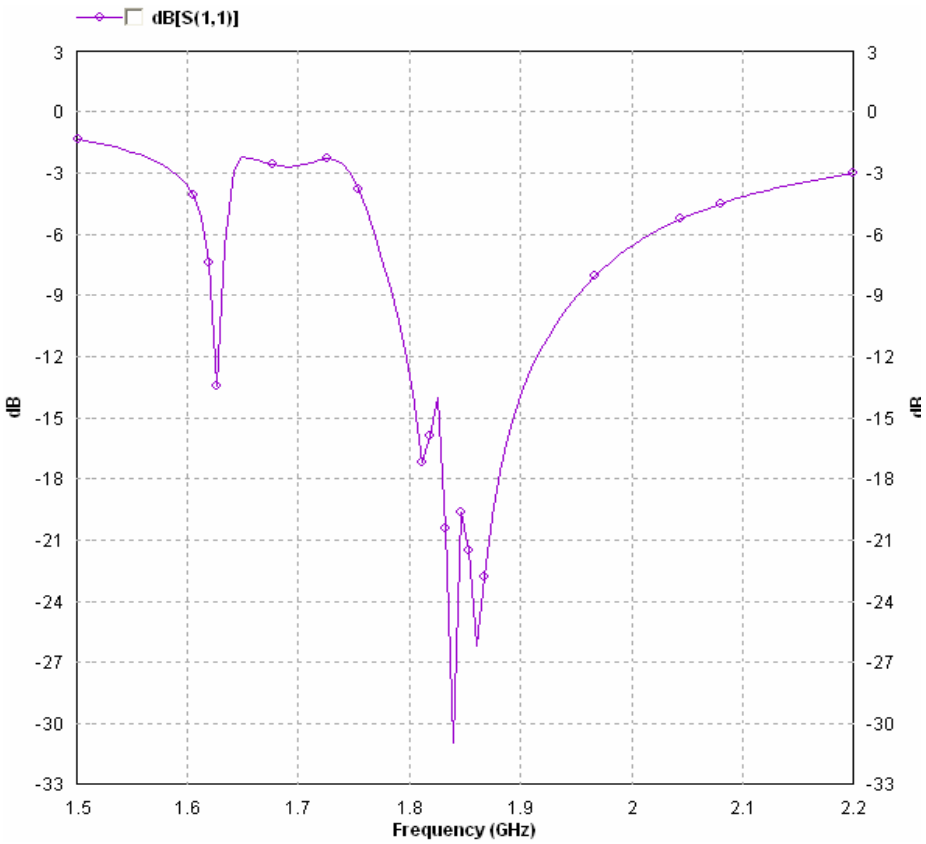

Figure 4.9: Return loss of Y- shaped and F-shaped antenna

Parameters: **(a)** L_1 = 31*mm*, L_2 = 14 *mm*, L_3 = 8 *mm*, L_4 = 1.5 *mm*, W_1 = 27 *mm*, W_2 = 10 *mm*, W_3 = 10 *mm*, W_4 = 5.5 *mm*, W_5 = 4 *mm*, W_6 = 2 *mm*, W_7 = 20 *mm*, xp = 16 *mm*, yp = 23 *mm*, xsp1 = 7.5 *mm*, ysp1 = 27 *mm*, xsp2 = 1.5 *mm*, ysp2 = 14 *mm*, r_p = 0.5 *mm*, r_{sp1} = 1 *mm*, r_{sp2} = 0.5 *mm*; **(b)** L_1 = 30 *mm*, W_1 = 28 *mm*

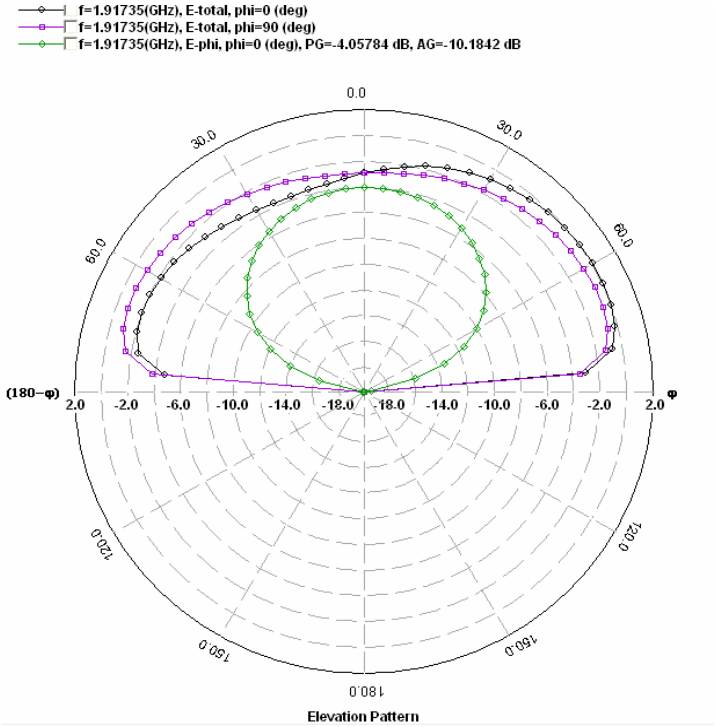

Figure 4.10: Far field radiation pattern of the stacked Y-shaped and F-shaped antenna

4.7 Comparison of the measured results and simulated results of the Interleaved F-shaped antenna

As mentioned before, the interleaved F-shaped antenna was fabricated and tested at the Royal Melbourne Institute of Technology (RMIT), Melbourne, Australia. Figure 4.11 shows the simulated and measured return loss of the proposed antenna for comparison. As mentioned in section 4.2, the simulated results were obtained using the *Zeland IE3D Commercial Software Package*. As can be seen from Figure 4.11, the -6 dB (3:1 VSWR) return loss bandwidth of the simulated and measured results are in good agreement excluding the resonance at about 2.42 GHz observed in the measured results. (Note that for wireless applications enabling devices, VSWR 3:1 is an acceptable definition for the operating bandwidth). However, the measured result degrades below -5 dB. This degradation could be due to the small fabrication tolerance associated with this antenna design. As can be seen from Figure 3.2, only a small gap (0.5 mm) separates the two F-shaped conductors. Moreover, if the etching is not perfect, degradation in the return loss characteristic is expected. Another tolerance limit is the location of the second shorting pin, i.e. (xsp2, ysp2). If the shorting is located even slightly over the edge, the return loss characteristic will degrade. As can be seen from the experimental results, there are two resonant frequencies, namely, at 1.85 GHz and 2.42 GHz. The bandwidth of the antenna is 7.1 % and 1% (3:1 VSWR) for the lower and higher resonance respectively. The presence of the second resonance in the measured results can be due to a finite size ground plane used in the measurements. IE3D assumes infinite size dielectric layers and ground plane.

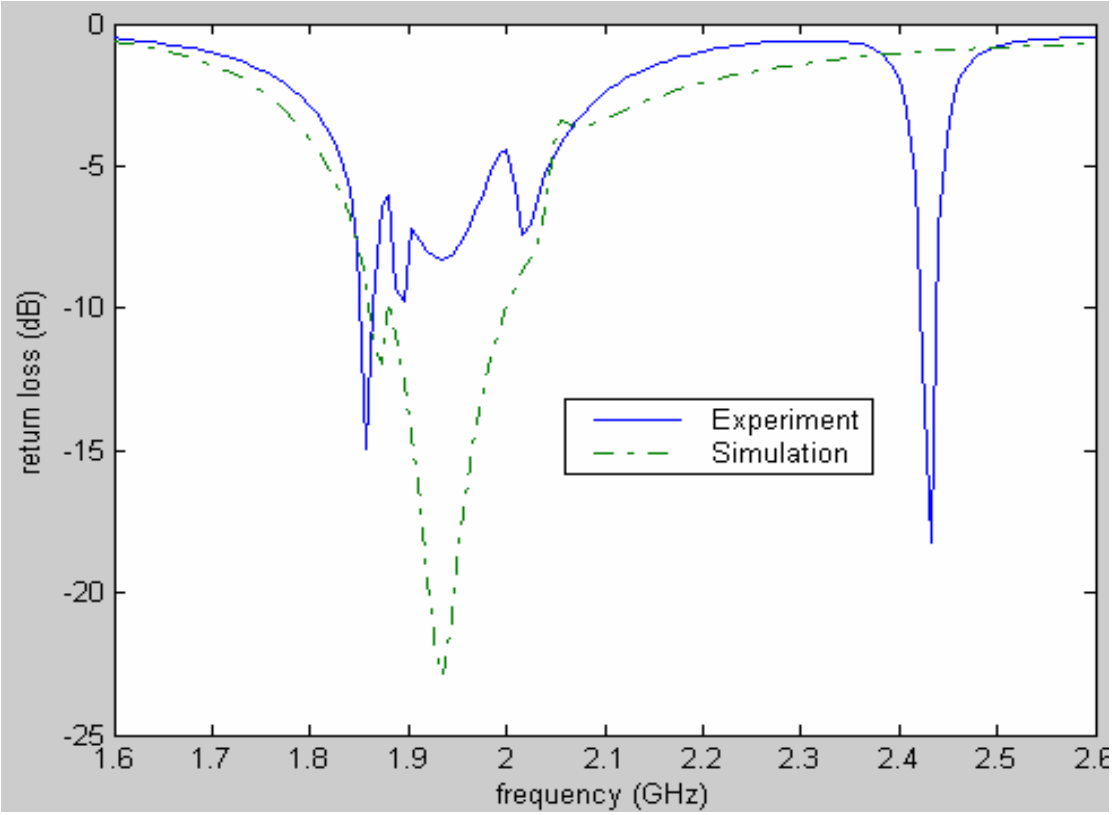

Figure 4.11: Simulated and experimental return loss behavior of the interleaved F-shaped antenna.

The far field radiation patterns of the interleaved F-shaped antenna printed antenna were measured at 1.85 GHz at the Royal Melbourne Institute of Technology anechoic chamber and are shown in Figure 4.12. The patterns show that the cross-polarization level in the E-plane is relatively high compared to the cross-polarization level in the H-plane (note that the broadside is 0 degrees on the plots). The co – polarization levels are literally omni-directional, which is similar compared to Figure 4.4. There are slight dips on the H-plane and can be seen at 70° and 280° on the plots. The measured gain of the antenna at the broadside is 1.6 dBi compared to 1.0 dBi from the calculated gain. The patterns in Figure 4.12 also show that the antenna radiates well at the back as well. The gain at the back of the antenna is 2.6 dBi.

The measured and simulated results are in good comparison to each other with slight differences. As mentioned before, these differences could be mainly due to the tolerance limits associated with this antenna. If the tolerance limits are minimized, then better antenna characteristics are expected. The return loss characteristics obtained from the experiment and the simulated results show that the antenna works well between 1.8 GHz and 2.0 GHz. The omni-directional radiation patterns obtained through experimentation and simulation tells that the antenna radiates well in all directions. This antenna is small enough to be used for PCS applications.

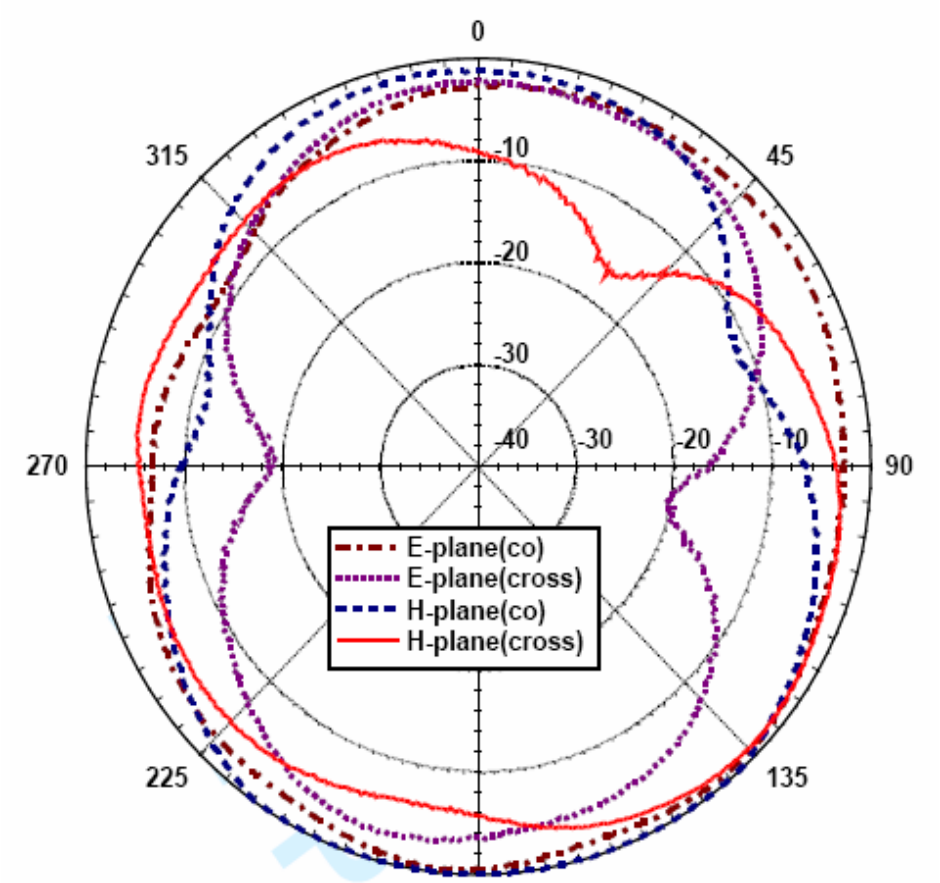

Figure 4.12: Measured radiation patterns at 1.85 GHz.

4.8 Concluding Remarks

Simulation results of five compact microstrip patch antennas have been presented in this section. The experimental results of the interleaved F-shaped antenna are also presented in this section to validate the design of the antenna using the *IE3D simulation package.* In section 4.2, the antenna conductor is Y-shaped and it has a stacked

configuration. The 10 dB return loss of this stacked antenna was 10.2 %. The overall dimension of the antenna was 31 mm x 27 mm. shorting pins and a shorting wall is utilized to reduce the size of the antenna.

The simulation result of the interleaved F- shaped antenna was presented in section 4.3. To further enhance the bandwidth of the antenna, a second F-shaped patch is electromagnetically coupled to a probe-fed F-shaped patch. The 10 dB return loss of the interleaved antenna was 7 %. The simulated gain of the antenna at this resonant frequency was 1 dBi at the broadside. The overall dimension of the antenna was 30 mm x 28 mm.

A third set of simulation results is presented in section 4.4 for the stacked interleaved F-shaped and cross-shaped antenna. The impedance bandwidth of the antenna determined from the 10 dB return loss was 10.5 % covering from 1.782 GHz to 1.981GHz. This relatively high bandwidth is compliant with most mobile devices. The simulated gain of the antenna is 0.9 dBi. This new antenna design has an overall size of 30 mm x 28 mm.

In section 4.5, the simulated return loss and far field radiation patterns of the stacked square shaped and cross-shaped antenna at 1.87 GHz was presented. The 10 dB return loss (VSWR> 2) is 8.4 %. The overall size of this antenna was 30 mm x 28 mm. In this antenna the current path is lengthened by incorporating the semi circular grooves on the top layer.

Finally, the simulation results of the stacked Y-shaped and interleaved F-shaped antenna were presented in section 4.6. The 10 dB return loss of this new design was 8.15 %. The overall size of the antenna was 31 mm x 28 mm.

In section 4.7, the experimental results of the interleaved F-shaped antenna were presented. Two resonant frequencies were produced at 1.85 GHz and 2.42 GHz. The bandwidth of the antenna was 7.1 % and 1% (3:1 VSWR) for the lower and upper frequency respectively. This experimental result showed a slight degradation in the return loss characteristic. This could be mainly due to tolerance limits such as the etching of the antenna and the precise location of the shorting pins. The measured gain of the antenna at the broadside was 1.6 dBi compared to 1 dBi from the calculated gain.

From these measured results it can be said that the *IE3D Zeland software* can indeed be used to design microstrip patch antennas. The results obtained through simulation for the 5 antennas presented here can be relied upon in terms of the return loss characteristics and the radiation patterns of the actual antenna. Slight differences in the experimental results could be due to the inevitable fabrication tolerances associated with the antennas. The 5 new antenna designs presented in chapter 3 can be used for mobile applications.

CHAPTER 5: CONCLUSION AND FUTURE RESEARCH

In this thesis, compact mobile antennas for mobile communications were investigated. The objectives of this research were to study some common size reduction techniques available in the literature and to determine the best methods of reducing the dimensions of a patch antenna through software analysis. Once these objectives were achieved, the next objective was to design new compact patch antennas by using an electromagnetic IE3D CAD simulator. The final objective of this research was to fabricate and experimentally test at least one antenna to validate the design of the antennas using the software package.

In chapter 2, discussions on most common methods of size reduction techniques were presented. These included the use of shorting pins, slots, high dielectric constant substrate materials, chip resistor loading, slow wave structure, and the use of a meandered ground plane. Analyses of these methods were also carried out to determine which methods gave the most percentage size reduction in terms of the linear dimensions of the antennas. The percentage size reduction and bandwidth was calculated with respect to a reference antenna operating in the L- band spectrum. A reference antenna is one in which no reduction method has been applied to. The dimensions of the reference antennas were as follows: rectangle – 74 mm (*Length*) x 32 mm (*Width*), triangle – 98 mm (*Length*) x 86 mm (*height*) and circle – 36 mm (*radius)*. Through several analyses, it was found that the best size reduction methods to reduce the antenna dimensions were to use shorting pins and slots on rectangular antennas. One drawback of using these techniques was that the bandwidth of the antennas also decreased with the decrease in the

size of the antennas. Therefore, some literature review was also carried out on the bandwidth enhancement techniques of microstrip patch antennas.

The in depth design of five new compact microstrip patch antennas was presented in chapter 3. The first design, a Y-shaped stacked antenna utilized the technique of introducing shorting pins, shorting wall and slots to reduce the overall dimension of a rectangular shaped antenna. The antenna consists of two patch layers, where the shape of both the layers had the same geometry. Two shorting pins were utilized in this configuration. To achieve a reasonable bandwidth, a parasitic ring was placed around the Y shape. The dielectric layers were separated by *Rohacell* foam of thickness 3 mm. Note that all the antennas were fed coaxially. The second interleaved F-shaped small antenna was designed and discussed. The antenna consists of two patches, namely, a right side up F-shaped fed patch and an electromagnetically coupled inverted F-shaped patch. Both the patches had one shorting pin to help reduce the overall size of the antenna. A parasitic ring enclosed the conductor patch. A *Rohacell* foam of thickness 6 mm was sandwiched between the conductor layer and the ground plane to increase the bandwidth of the antenna. Another stacked antenna was presented where the top layer was interleaved F-shaped (as discussed above) and the bottom layer was cross-shaped. The cross- shaped patch lengthened the current path and enabled a third resonance. The conducting planes were separated by *Rohacell* foam of thickness 3 mm. This bottom layer had a feed pin and a shorting pin, from the top patch, extending to the ground plane. The fourth antenna design was a stacked square and cross-shaped microstrip patch antenna. The square shape utilized the semi circular grooves technique used in [47] to decrease the size of the printed conductor. These grooves were placed on the four sides of the square to

effectively lower the resonant frequency of the modified patch. This is done by maximizing the current path. One shorting pin was placed in close proximity to the probe pin to further reduce the size of the antenna. As mentioned before, several radiating slots on the cross – shaped patch in the second layer was used to increase the current patch and hence reduce the dimensions of the antenna. Once again the conducting layers were separated by *Rohacell* foam of thickness 3 mm. Finally, a small stacked Y-shaped and interleaved F-shaped antenna was designed and discussed in chapter 3. This design used 2 shorting pins to help reduce the antenna dimensions. A parasitic ring enclosed the radiating patches in both the layers to improve the bandwidth of the antenna. Placing 3 mm thick foam materials between the conducting layers also enhanced the antenna bandwidth.

The simulation results of the five new compact antennas were presented in chapter 4. The Y-shaped stacked antenna operates from 1.8 GHz to 2 GHz with a bandwidth of 200 MHz. The 10 dB return loss of the antenna was 10.2 %. The gain of the antenna at the broadside was calculated to be –1.7 dBi. The overall dimension of the antenna was 31 mm x 27 mm. The interleaved F-shaped antenna operates from 1.864 GHz to 2 GHz. The 10 dB return loss bandwidth of the antenna was 140 MHz, achieving a bandwidth (VSWR >2) of 7 %. The simulated gain of the antenna at 1.88 GHz was 1 dBi at the broadside. The total radiation at $\phi = 0$ degrees is almost omni – directional about the broadside. The size of this antenna was 30 mm x 28 mm. To validate the design using the software package, this antenna was also fabricated and tested. Two resonant frequencies were excited. The measured return loss was obtained to be 7.1 % and 1 % (3: 1 VSWR) for the lower and upper resonance respectively. The measured and simulated

results are in good agreement below the -5 dB return loss. The results depict that by using the IE3D simulation package; the designs presented in chapter 3 are valid and hence can be used in mobile communications. Note that the results degrade below 5 dB. This could be due to fabrication tolerance such position of the shorting pin and the exact etching of the conducting planes.

The predicted return loss of the interleaved F-shaped and cross-shaped stacked antenna was 10.5 %, covering from 1.782 GHz to 1.981GHz. This is a reasonably high bandwidth and is compliant with most systems such as DCS 1800 (1805 MHz-1880 MHz), Digital European Cordless Telephone (1880 MHz-1990 MHz), Personal Handy Phone System (1895 MHz-1918 MHz) and PCS systems. The simulated gain was 0.9 dBi. The radiation patterns were almost omni – directional in the plane $\phi = 0$ degrees. The interleaved F-shaped and cross – shaped stacked antenna had an overall size of 30 mm x 28 mm. The simulated return loss of the fourth antenna, the square and cross-shaped stacked, antenna was 8.4 %. The size of this antenna (L = 30 mm, W = 28 mm) was 65 % smaller than a standard probe fed rectangular printed antenna. Conventional patch antennas have a very small bandwidth, typically 1 %. The simulated gain was obtained to be 0.6 dBi. The fifth antenna, the Y-shaped and interleaved F-shaped antenna had a bandwidth of 8.15%, covering from 1.79 GHz to 1.938 GHz. A 63% patch size reduction from the conventional probe fed rectangular patch antenna was observed. The simulated gain of this antenna at 1.92 GHz was – 0.9 dBi. The antenna is compact and small with the overall size of the antenna being 31 mm x 28 mm.

5.1 Suggestions for Future Work

Five new compact microstrip patch antennas have been proposed here. One antenna has been fabricated and tested to valid the simulation results. A suggestion for future work would be to carry out the investigation of the other four antennas and compare their results. The fabrication tolerance of these antennas must be kept in mind when comparing the simulation and measured results.

Another future activity would be to incorporate these antennas in actual handsets or mobile devices to determine how well these antennas work in practical situations.

REFERENCES

[1]. Huie, K. C., "Microstrip patch antennas: broadband radiation patterns using photonic crystal substrates", M.Sc Thesis, *Virginia Polytechnic Institute and State University,* Jan. 11, 2002.

[2]. Balanis, C. A., "Antenna theory: analysis and design", 2nd edition, John Wiley & Sons, Inc., New York, 1997.

[3]. Agarwal, P. K. and Bailey, M. C., "An analysis technique for microstrip patch antennas"*, IEEE Trans. Antennas and Propagation, Vol. AP-25, No. 6, pp. 756 - 759, 1977.*

[4]. IE3D simulator, Zeland Software, 2005.

[5]. Lal, J., Kan, H. K., Rowe, W., and Chung, K. L., "F-shaped shorted patch antenna with dual – frequency characteristics"*, accepted to* Microwave & Optical Technology Letters*, April.*

[6]. Lal, J., and Kan, H. K., "Cross-shaped shorted patch antenna", *2005 Proc. Asia Pacific Microwave Conference,* Suzhou, China, Vol 3, pp. 1 – 4, December 2005.

[7]. Wong, K.L., Compact and broadband microstrip antennas, John Wiley & Sons Inc., New York, 2002.

[8]. Gardiol, F. E., and Zurcher, Jean-Francois, "Broadband patch antennas", *Artech House Publishers*, June 1995.

[9]. Pozar, D. M., and Schaubert, D., "Microstrip antennas: The analysis & design of microstrip antennas & arrays", *Wiley – IEEE press*, May 1995.

[10]. Bancroft – Randy, "Microstrip and printed design', *Noble Publishing Associates*, April 2004.

[11]. Waterhouse, R.B., Targonski, S.D., and Kokotoff, D. M., "Design and performance of small printed antennas*", IEEE Trans. Antennas and Propagation,* Vol. 46, pp. 1629 – 1633, 1998.

[12]. Denidni, T. A., "Design of a wideband microstrip antenna for mobile handset applications", *High Frequency Electronics*, pp. 24 – 28, February 2004.

[13]. Gosalia, K. and Lazzi, G., "Reduced size, polarized microstrip patch antenna for wireless communications", *IEEE Trans. Antennas and Propagation*, Vol. 51, No. 9, pp. 1629 – 1633, Sept. 2003.

[14]. Sze, J. Y. and Wong, K. L., "Slotted rectangular microstrip antenna for bandwidth enhancement," *IEEE Trans. Antennas and Propagation*, Vol. 48, No. 8, pp. 1149 – 1152, Aug. 2000.

[15]. Dey, S. and Mittra, R., "Compact microstrip patch antenna"*, Microwave Optical Technol. Lett.* 13, pp. 12 – 14, Sept. 1996.

[16]. Chrissoulidis, D. P., Liakou, P. C., and Notis, D. T., "Dual polarized microstrip patch antenna, reduced in size by use of peripheral slits", *Department of Electrical & Computer Eng., Aristotle Uni. of Thessalonica*, Greece.

[17]. Colburn, J. S and Samii. Y. R., "Patch antennas on externally perforated high dielectric substrate", *IEEE Trans. Antennas and Propagation*, Vol. 47, No. 12, pp. 1785 – 1794, Dec. 1999.

[18]. Y. Qian, R. Coccioli, D. Sievenpiper, V. Radisic, E. Yablonovitch, T Itoh, "Microstrip patch antenna using novel PBG structures", *Microwave Journal*, Vol. 42, No. 1,pp. 66 – 76, 1999.

[19]. Lin, Y. F. and Wong, K. L., "Small broadband rectangular microstrip antenna with chip resistor loading", *Electron. Letters,* 33, pp. 1593 – 1594, 1997.

[20]. Lu, J. H., "Broadband operation of a slot coupled compact rectangular microstrip antenna with a chip resistor loading", *Proc. Natl. Sci. Counc.*, Vol. 23, No. 4, pp. 550 – 554, 1999.

[21]. Yang, F. R., "A novel low – loss slow – wave microstrip structure", *IEEE Microwave Guided Wave Lett*., Vol. 8, no. 11, pp. 372 – 374, Nov. 1998.

[22]. Azadegan, R., Harvey, J., Mosallaei, H., and Sarabandi, K., "Antenna miniaturization techniques for applications in compact wireless transceivers", *Department of Electrical & Computer Eng.,* Uni. of Michigan.

[23]. Fries, M. K. and Vahldieck, R., "Small microstrip patch antenna using slow wave structure", *Swiss Federal Institute of Technology*, Zurich, Switzerland.

[24]. Antar, Y.M.M and Collins S., "Single elements and arrays with a reduced ground plane size", *Royal Military College of Canada.*

[25]. Alam, M., and Bornemann, J., Rambabu, K., and Stuchly, M. A., "Compact wideband dual-polarized microstrip patch antenna", *Dept. of Electrical & Computer Engineering*, University of Victoria, 2004.

[26]. Anandan, C. K., Kuntukulam, S. O., Paulson, M., and Mohanan, P., "Arrow-shaped microstrip antenna for broadband operation", *Centre for Research in Electromagnetics & Antennas, Dept. of Electronics*, Cochin Uni. Of Science & Tech., India.

[27]. Ali, M., Dougal, R., Hwang, H., and Yang, G., "Wideband circularly polarized microstrip patch antenna for wireless LAN applications", *Department of Electrical Engineering*, Uni. Of South Carolina, Columbia.

[28]. Lin, C. K., and Wang, Y. J., "Design of dual-frequency microstrip patch antennas and application for IMT-2000 mobile handsets", *Progress in Electromagnetics Research*, PIER 36, pp. 265-278, 2002.

[29]. Ollikainen, J., Fischer, M., and Vainikainen, P., "Thin dual – resonant stacked shorted patch antenna for mobile communications", *Electron. Lett.,* 35, pp. 437 – 438, March 18 1999.

[30]. Wong, K. L and Yang. K. P., "Modified planar inverted F antenna", *Electron. Lett.,* 34, pp. 6 – 7, Jan. 8, 1998.

[31]. Wong, K. L. and Wu, C. K., "Broadband microstrip antenna with directly coupled and gap – coupled parasitic patches", *Microwave Opt. Technol. Lett.*, 22, pp. 348 – 348, Sept. 5, 1999.

[32]. Gupta, K. C., and Kumar, G., "Non-radiating edges and four edges gap-coupled multiple resonator broad-band microstrip antennas", *IEEE Trans. Antennas and Propagation*, Vol. AP-33, No. 2, pp. 173 – 178, February 1985.

[33]. Erdemli, Y. E., Gilbert, R. A., Sertal, K., Wright, D. E., and Volakis, J. L., "Frequency selective surface to enhance performance of broadband reconfigurable arrays", *IEEE Trans. Antennas and Propagation*, Vol. 50, No. 12, pp. 1716 – 1724, Dec. 2002.

[34]. Aberle, J. T., Kokotoff, D. M., and Waterhouse, R. B., "Rigorous analysis of probe-fed printed annular ring antennas", *IEEE Trans. Antennas and Propagation*, Vol. 47, No. 2, pp. 384 – 388, February 1999.

[35]. Chiou, C. W., Tang, C. L., and Wong, K. L., "Broadband dual – frequency V – shape patch antenna", *Microwave Opt. Technol. Lett.*, 25, pp. 121 – 123, April 20 2000.

[36]. Murch, R. D. and Rowell, C. R., "A capacitively loaded PIFA for compact mobile telephone handset", *IEEE Trans. Antennas and Propagation*, Vol. 45, pp. 837 – 842, May 1997.

[37]. Bhat, B., Gupta, V., Koul, S. K., and Sinha, S., "Wideband dielectric resonator loaded suspended microstrip patch antennas", *Microwave and Optical Technology Letters,* Vol. 37, No. 4, pp. 300 – 302, May 20, 2003.

[38]. Yang, H. Y., "Miniaturized printed wire antenna for wireless communications", *Department of Electrical and Computer Engineering*, University of Illinois, Chicago.

[39]. Lee, K. F and Lee, R. Q, "Gain enhancement of microstrip antennas with overlaying parasitic elements", *Electron. Lett.,* 24, pp. 656 – 658, Jan. 8, 1988.

[40]. *Porath, R., "Theory of miniaturized shorting – post microstrip antennas",* IEEE Trans. Antennas and Propagation*, Vol. 48, No. 1, pp.41 – 47, January 2000*

[41]. Chair, R., Guo, Y. X., Hawkins, J. A., Lee, K. F, and Luk, K. M., "Theory and experiment on microstrip patch antennas with shorting walls", *IEE Proceedings Microw. Antennas Propagat*., 147, pp. 521 – 525, 2000.

[42]. Mahmoud, S. F., Mohra, A., and Sheta, A. F., " Multi – band operation of a compact H – shaped microstrip antenna", *Microwave and Optical Technology Letters,* Vol. 35, No. 5, pp. 363 – 367, December 5, 2002.

[43]. Deshmukh, A. A., and Kumar, G., "Compact broadband C – shaped stacked microstrip antennas", AP – S Symp. Digest, Vol, 2, pp. 538 – 541, June 2002.

[44]. Rahmat – Samii, Y., Yang, F., Ye, X., and Zhang, X. X., "Wide – band E – shaped patch antennas for wireless communications"*, IEEE Trans. Antennas and Propagation, Vol. 49, pp.1094 – 1100, July 2001.*

[45]. Kan, H. K., "Small printed antennas for wireless communication handset terminals, PhD Dissertation, *School of Electrical and Computer Engineering,* RMIT, Australia, November 2001.

[46]. Wood, C., " Improved bandwidth of microstrip antenna using parasitic elements, *IEE proceedings,* Vol. 127, pp. 231 – 234, 1980.

[47]. Gupta, N., and Gupta, V. R., "Characteristics of a compact circularly polarized antenna", *Dept. of Electronics & Communication Engineering*, Birla Inst. Of Technology, Ranchi, India, pp. 10 – 12.

[48]. Florida State University, ETD collection, http://etd.lib.fsu.edu/thesis/available/etd-04102004-143656/unrestricted/Chapter4.pdf

[49]. Hong, C-S., "Gain – enhanced broadband microstrip antenna", *Proc. Natl. Sci. Counc. ROC(A)*, Vol. 23, No. 5, pp. 609 – 611, 1999.

[50]. Huynh, T., Lee, K. F., Lee, R. Q., Luk, K. M., Tong, K. F., and Shum, S. M., "Experimental and simulation studies of the coaxially fed U-slot rectangular patch antenna," *IEEE Proceeding Microwave Antennas Propagation,* 144, pp. 354-358, Oct. 1997.